CH and C_2 Measurements Imply a Radical Pool within a Pool in Acetylene Flames

Keith Schofield* and Martin Steinberg†

Materials Research Laboratory, University of California, Santa Barbara, California 93106-5121

Received: October 14, 2006; In Final Form: January 12, 2007

Measured CH and C_2 profiles show a striking resemblance as a function of time in a series of seven well-characterized fuel-rich ($\phi = 1.2-2.0$) non-sooting acetylene flames. This implied commonality and interrelationship are unexpected as these radicals have dissimilar chemical kinetic natures. As a result, a rigorous examination was undertaken of the behavior of each of the hydrocarbon species known to be present, C, CH, CH_2, CH_3, CH_4, CHO, CHOH, CH_2O, CH_2OH, CH_3O, CH_3OH, C_2, C_2H, C_2H_2, CHCO, CH_2CO, and C_2O. This emphasized the main region where CH and C_2 are observed (50−600 μs) and reduced the kinetic reactions to only those that operate efficiently and are dominant. It was immediately apparent that this region of the flame reflects the nature of a hydrogen flame heavily doped with CO and CO_2 and containing traces of hydrocarbons. The radical species, H, OH, O, along with H_2, H_2O, and O_2, form an important controlling radical pool that is in partial equilibrium, and the concentrations of each of the hydrocarbon radicals are minor to this, playing secondary roles. As a result, the dominant fast reactions are those between the hydrocarbons and the basic hydrogen/oxygen radicals. Hydrocarbon−hydrocarbon reactions are unimportant here at these equivalence ratios. CH and C_2 are formed and destroyed on a sub-microsecond time scale so that their flame profiles are the reflection of a complex kinetically dynamic system. This is found to be the case for all of the hydrocarbon species examined. As might be expected, these rapidly form steady-state distributions. However, with the exceptions of C, CHO, CHOH, and CH_2O, which are irreversibly being oxidized, the others all form an interconnected hydrocarbon pool that is under the control of the larger hydrogen radical pool. The hydrocarbon pool can rapidly adjust, and the CH and C_2 decay together as the pool is drained. This is either by continuing oxidation in less rich mixtures, or in richer flames where this is negligible by the onset of hydrocarbon−hydrocarbon reactions. The implications of such a hydrocarbon pool are significant. It introduces a buffering effect on their distribution and provides the indirect connection between CH and C_2. Moreover, because they are members of this radical pool, flame studies alone cannot answer questions concerning their specific importance in combustion other than their contributing role to this pool. The presence of such a pool modifies the exactness that is needed for kinetic mechanisms, and knowledge of every species in the system no longer is necessary. Furthermore, as rate constants become refined, it will allow for the calculation of the relative concentrations of the hydrocarbon species and facilitate reduced kinetic mechanisms. It provides an explanation for previous isotopically labeled experiments and illustrates the difficulty of exactly identifying in flames the role of individual species. It resolves the fact that differing kinetic models can show similar levels of accuracy and has implications for sensitivity analyses. It finally unveils the mechanism of the flame ionization detector and has implications for the differing interpretations of diamond formation mechanisms.

I. Introduction

CH and C_2 are well-established ubiquitous radicals in fossil fuel combustion. They have a rich spectroscopy and have been studied from the earliest of days, initially mainly due to their chemiluminescent nature. Despite innumerable studies, their roles and relationships in the general chemical kinetics of combustion remain unknown. The participation of CH in "prompt" NO formation[1] and in chemi-ionization[2] now is accepted, and kinetic modeling of observed CH concentration profiles is becoming reasonably adequate in methane fueled flames.[3] Much less is known of the nature of C_2. Mainly due to a lack of reaction rate data, it has never been included in any of the large kinetic modeling databases created for fuels such as methane or acetylene.[4−8] A cursory effort was made to do this by Bernstein et al.,[9] but no measurements were made. Recently, Smith et al.[10] similarly added several reactions of C_2 to GRI-Mech 3.0 but were emphasizing the comparison of its ground- and excited-state populations. The latest effort by Brockhinke et al.[11] obtained the profile of C_2 in a single low-pressure $\phi = 1.5$ propene flame, but initial attempts to model this were not fruitful. Consequently, as with other trace species, concentrations and profiles are obtained, but no questions are answered concerning whether the species is playing an important role or not. In discussions in recent years, such questions have been resurfacing as to whether CH or C_2 may be involved in soot formation or play a pivotal role in flame diamond deposition. Many years ago, the first elegant isotopically labeled experiments of Ferguson[12] indicated that excited C_2(d) in acetylene flames is formed from two single carbon fragments. Yet even now its exact formation mechanism remains speculative.[10] Also, since that time many other interesting ^{13}C-, ^{14}C-,

* Corresponding author. Phone: (805) 966-6589. Fax: (805) 965-9953. E-mail: combust@mrl.ucsb.edu

† Retired.

10.1021/jp0667689 CCC: $37.00
Published on Web 02/28/2007

and D-labeled fuel experiments have been reported that remain unexplained. Twenty years ago, by monitoring C_2 in absorption with a low-pressure C_2H_2/N_2O flame, Darian and Vanpee[13] concluded as had Gaydon and Wolfhard[14] that a reasonable fraction of the flame carbon seemed to transfer through this radical. Whether this is true or not still has not been answered. For these and other reasons, it was decided to examine the chemical kinetic behavior of CH and C_2 by monitoring their ground-state concentrations along with those of OH and H in a series of well-defined and characterized fuel-rich acetylene flames. Its main aim was not to improve kinetic models or suggest new modeling techniques but rather to understand the basic relationship between these two radicals and establish their roles. As will be seen, the implications of the measurements, coupled to simple kinetic considerations, have provided a fundamentally rich grasp of the interplay between all of the basic hydrocarbon species in the flame zone immediately adjacent to the reaction zone. This initial paper presents the experimental data and the logical analysis that lays the foundation for this new insight.

II. Previous Measurements of CH and C_2 in Flames

CH, C_2, OH, and H, the species measured in this program, all overshoot their thermodynamic equilibrium concentrations in the reaction zone of premixed fuel-rich hydrocarbon flames and decay toward equilibrium in the post-flame gases. For OH and H, the overshoots are several orders in magnitude, and their chemistry is such that decay is relatively slow due to kinetic constraints on recombination. As a result, they can extend for many milliseconds in a fast burning flame at atmospheric pressure. C_2 and CH at equilibrium should not exist in these flames ($<10^{-12}$ mole fraction), so any observation is a significant overshoot, and in this case their decay generally is rapid. Many measurements of CH or C_2 concentrations have been reported in a wide variety of flames burning alkane, alkene, and acetylene fuels.[15] However, due to the fact that by adjusting either fuel type or conditions their concentrations can be tailored to a low ppmv scale, the main emphasis often has centered more on such flames representing a convenient source of these radicals. As a result, over the years, this has provided a means for testing any new analytical monitoring technique and has been used to establish sensitivity limits. Little has emerged from such studies concerning flame chemistry. Nevertheless, fortunately there have been several quantitative studies that have examined their specific natures in a variety of flames. Of these, even fewer have simultaneously monitored both radicals. Generally, what has been established is that their concentrations are vanishingly small in oxygen-rich flames but increase significantly for stoichiometric and larger equivalence ratios. Also, their peak levels are largest in acetylene flames and decrease with increasing bond saturation of the fuel.

For C_2, seven quantitative absorption studies have been reported in acetylene flames. These generally have used the strong $d^3\Pi_g-a^3\Pi_u$ (0,0) band originating from its low-lying electronically excited state.[13,16−21] To convert these measurements to an absolute C_2 concentration requires the temperature of the lower state and an assumption of an equilibrated distribution over the rotational, vibrational, and electronic manifolds of the partition functions, which does appear to be the case certainly for this $a^3\Pi_u$ state.[20] Although $a^3\Pi_u$ lies 612 cm^{-1} above the $X^1\Sigma_g^+$ ground state, at flame temperatures it will represent about 80% of the C_2 population due to its degeneracy and as shown later is equilibrated with the ground state at atmospheric pressure within a microsecond. A re-examination of these absorption studies that used fuel-rich C_2H_2/O_2 or N_2O flames of equivalence ratios from 0.8 to 3.3 and pressures from 2.6 mbar to atmospheric pressure shows reasonable agreement, indicating peak concentrations of the order 60−180 ppmv. None illustrate the effects of equivalence ratio on the C_2 flame profile, but Bulewicz et al.[20] do show the variation of the peak density. Two additional studies obtained flame profiles for C_2 using LIF.[22,23] Of these, the latter[23] noted also that its concentrations in a stoichiometric acetylene flame can be at least 1−2 orders of magnitude larger than the corresponding measures with CH_4, C_2H_6, or C_2H_4 fuels. The similar smaller variations between these latter three fuels have also been reported with equivalence ratios of 1.01 and 1.28.[10]

Also dominant under fuel-rich conditions, CH concentration levels have been measured more extensively than for C_2 and for equivalence ratios as low as 0.4 and well into sooting flames with a value of 3.3. Concentrations are at least 3-fold larger in stoichiometric acetylene flames than in less unsaturated fuels that are all very similar.[23] This rather invariant behavior in CH_4, C_2H_6, or C_2H_4 flames now has been confirmed.[9,10] For acetylene flames, profiles are again short-lived and indicate concentrations of about 10−100 ppmv. There is a slight pressure and temperature dependence,[24] but all measurements obtaining concentration profiles through the flame have been made at reduced pressures of from 3 to 130 mbar (2−100 Torr).[18,20,21,23−28] Of these studies, four with reduced pressure acetylene flames did obtain profiles of both CH and C_2.[18,20,21,23] More will be said later of this prior body of work in connection with the new data presented herein, and on the previous limited efforts to kinetically model the observed profiles, which have mainly emphasized CH measurements in CH_4 flames.

It is because of these basic facts, together with acetylene's faster burning velocity, that C_2H_2 was chosen as the preferred fuel system for this study. Also, the use of flat flame atmospheric pressure burners provides well-defined spatial/time resolution with which to examine kinetic rates in a controlled flame environment.

The last 25 years has seen very significant efforts to develop generic chemical kinetic combustion models for the numerous fuels that are used in a multitude of combustion modes.[29,30] It has been driven mainly by continuing environmental concerns with pollutants and also with the increasing introduction of alternate fuels. Not surprisingly, this has led to mechanisms with reaction schemes that can include large numbers of species and many hundreds of reactions.[4−8,31−33] Because of the resulting computational limitations of trying to couple such chemical kinetics into computational fluid dynamic models, this has seen the introduction of numerous innovative mathematical methods for simplification. Generally, these are based on the separation of reactions according to their time constants and invoking steady-state methods. These are the so-called Intrinsic Low-Dimensional Manifold[34−37] or the Computational Singular Perturbation[38−40] approaches or other more recent emerging reduced model concepts.[41,42] In a few of the modeling attempts with acetylene, pictorial reaction networks outline the numerous reactions interconnecting the many species.[5,7,43] Of the two species of interest to the present study, only CH is considered. The models suggest that CH is either one step away from final oxidation or may with C_2H_2 be a building block for *c*-C_3H_2. Overall, it does not appear to be too interesting. One is left concluding that hydrocarbon combustion is a rather chaotic jumble of coupled reactions all rushing toward oxidation that can only be comprehended as sets of species whose concentrations have individual time profiles. Roles, interconnections, or

relationships between species appear to be but fleeting steady-state distributions that bear little meaning. Consequently, although models have yet to examine minor species such as CH and C_2 in any significant detail due to the lack of sufficiently accurate rate constants, the general consensus tends to suggest that in most situations their roles may be of little significance.

III. Hints of an Underlying Simplicity

Although a general atmosphere of complexity is conveyed by previous flame studies, there are somewhat unconnected observations that have been reported for a long time that hint that this may not be so. The flame ionization detector (FID) now has been a commercial instrument for almost 50 years.[44,45] It is a very effective measure of gas-phase total carbon in a stream of mixed hydrocarbons. It integrates and essentially counts carbon atoms to a good approximation.[46−49] It is widely used, but the full details as to how and why it actually works so well still are not fully understood! Generally, it is accepted that the organic molecule breaks down to CH_4 in the small pure-hydrogen diffusion flame that burns in air. This then produces CH radicals and chemi-ionizes by the reaction sequence:[2,50]

$$CH + O = HCO^+ + e^-$$

$$HCO^+ + H_2O = H_3O^+ + CO$$

The flame ions are H_3O^+ and electrons, the latter being monitored quantitatively. The surprising discovery, which has never fully received the credit deserved, was that the number of electrons produced correlates almost linearly with the quantity and number of carbon atoms in the hydrocarbon. If a concentration of methane produces a certain electron signal, a similar molecular concentration of toluene or heptane will show a 7-fold enhanced signal, cyclopentane about 5-fold, and ethylene 2-fold. In other words, there has to be a certain underlying simplicity whereby all hydrocarbons on combustion produce CH in a linear proportion to their carbon content. This appears to be a largely forgotten observation that has to contain significant implications for combustion and kinetic modeling. No kinetic modeling has yet resolved this occurrence satisfactorily. Nicholson[51] modified the model initially suggested by Blades[49] in which the hydrocarbons are all either initially H-atom cracked or pyrolyzed to CH_4 in the narrow pre-heating zone upstream of the flame front. More recently, Holm and Madsen[52−54] conclude that they have resolved the mechanism as a hydrogenolysis of the hydrocarbon to methane. However, none of the models are fully satisfactory and fail to explain how the further steps to CH remain a linear process and are not modified by further reduction to C-atom. Moreover, the creative experiments of Wagner et al.[55] effectively ruled out all of these mechanisms. They interchanged the flow lines so that the hydrocarbon sample was injected into an air jet that burned in a cloud of hydrogen. Sensitivity was reduced, but the relative responses and the linearity remained unchanged. Consequently, the explanation has to lie in the combustion mechanism itself.

A second feature of numerous organic molecules is their apparent ease on fragmentation of producing C_2. This has been known for a long time, having been noted in shock tube pyrolysis of organics, C_{60}, and acetylene.[56−58] It has also been seen, for example, in many multiphoton absorption experiments with molecules such as C_2H_3Cl, $C_2H_5NH_2$, or C_6H_6.[59] C_2 can be a primary product of such fragmentations. Moreover, at higher pressures even CH_3OH will produce C_2.[59] This is especially intriguing as methanol is one fuel that is not easily prone to combustion-produced soot formation.[14] Also, the C_2 formed in the photofragmentation of benzene or C_2H_2 appears on a picosecond time scale and in the latter case is the result of a rapid two-step process via C_2H.[60,61] Photodissociation of the molecule CF_3OOCF_3 even manages to produce C_2.[62] Also, as reported in several LIF measurements of C_2 in flames, extra care must be taken particularly in near- or sooting conditions if it is to remain a non-intrusive monitor. Depending on the laser wavelength and fluence, it is easy to produce C_2 in the burned gases from either the soot or some other carbon radical.[22,63,64] The latter study[64] also noted nascent C_2 in the vicinity of the burner, indicating a rapid prompt-type formation and growth. The significant thermodynamic stability particularly of C_2 is undoubtedly a driving force in some of this chemistry, the bond strengths of these radicals being $D_0(C_2) = 608$ and $D_0(CH) = 335$ kJ mol^{-1}.

A very relevant and important observation was made by Chou and Dean.[65] With an original and very novel technique at the time, they used a high-power ArF laser at 193 nm to perturb the burned flame gases. The laser pulsed rich ($\phi = 1.6-1.8$) atmospheric pressure CH_4 flames, and then a probe laser monitored the time-resolved decay of the enhanced concentrations of the CH radicals that had been created. These were seen to recover with a decay lifetime (1/e) of about 5 μs. This indicated that very fast removal kinetics was involved; yet the normal flame CH concentrations could extend at least 40-times longer. The only conclusion to be drawn was that CH is constantly being formed and destroyed throughout these burned gases. Moreover, as will be seen later, the chemical quenching rates for CH now are known to be even faster than 5 μs, and why the perturbation lasted as long as it did has intriguing implications.

Because, taken together, such aspects obviously seem to be conveying some basic behavioral information, it was decided to monitor C_2 and CH concentration profiles as a function of time in a series of seven fuel-rich acetylene flames, and also to use flames that could be well characterized concerning their basic temperatures and H, H_2, OH, O, O_2, CO, CO_2, and H_2O flame concentration profiles.

IV. Experimental Methods

A flat-flame front atmospheric pressure Padley−Sugden-type burner was used.[66] Flows produced a cylindrical one-dimensional laminar flame that consisted of an inner experimental flame into which additives might be made, surrounded by an otherwise identical flames. This outer flame helps to maintain the inner flame shape over many centimeters length, improves stability, and removes any perturbing edge effects. The circular cross-section inner-core flame, burned vertically, has a uniform temperature and concentration across its diameter of about 11 mm. Radial diffusion generally is minimal and neglected at atmospheric pressure. Premixed gases are controlled by mass flow meters and in the present study involved a matrix of seven fuel-rich $C_2H_2/O_2/N_2$ mixtures that burned soot-free with equivalence ratios of 1.2, 1.6, and 2.0. A stoichiometric mixture for an acetylene flame contains C_2H_2/O_2 in the unburned gas volume ratio of 1:2.5. Flame temperature is controlled by the ratio of N_2 used. The seven flames burned had unburned volume ratios of $C_2H_2/O_2/N_2$ of 1.2/2.5/10, 1.2/2.5/12, 1.2/2.5/14, 1.2/2.5/16, 1.6/2.5/10, 1.6/2.5/12, and 2.0/2.5/10. Temperatures for these fell in the range 1750−2450 K, and a combustion time of 0.25 ms corresponded to downstream distance flame lengths of about 1.1−3.1 mm. Because of the short-lived nature of the hydrocarbon radicals in these burned gases, measurements

emphasized the 0.1−0.5 ms region in most flames but did extend to 1.5−2.5 ms in the richest flame examined. A fuel-rich $H_2/O_2/N_2$ (4/1/2 unburned volume ratios) containing 1% SO_2 also was used to facilitate an absolute calibration of the laser-induced fluorescence (LIF) measurements of OH concentrations. It was previously confirmed at 2 ms downstream in such a 2400 K flame that the OH concentration is at its equilibrium value and so provides a convenient scalar.[67] The burner was mounted on a computerized platform driven by a stepped motor that could accurately raise or lower it relative to the optical axis. Fluorescent radiation from the flame is collected on a two-mirror rotator that images a horizontal slice of the flame at flame center into the vertical entrance slit (50 μm wide by 0.5 cm high) of a monochromator. This spectrometer is sufficient to resolve rotational structure and also defines the flame spatial resolution of about 0.1 mm, or with these flames, times of about 0.01−0.02 ms. For very low spectral intensities, slit widths could be increased with only slight loss of spatial resolution.

When needed, an ultrasonic nebulizer injected small quantitative additions of a fine aerosol of an aqueous salt solution into the inner flow gases. Solutions of $NaNO_3$ and $LiNO_3$ were used for sodium D-line reversal measurements of temperature, and for Na/Li atomic emission comparison measurements of H-atom concentrations,[68] as validated previously in a series of $H_2/O_2/N_2$ flames.[66] The burner and flow lines were heated to minimize any condensation or deposition.

The major experimental measurements have centered on monitoring absolute OH concentrations and relative C_2 and CH concentrations using laser-induced fluorescence (LIF) techniques. The same method as validated in previous studies was repeated for OH.[66,67,69] The OH(A-X), (1,0) $R_1(6)$ line at 281.14 nm was excited, and the fluorescence intensity was monitored of the (1,1) $Q_1(7)$ line at 314.69 nm. In a low laser power mode, the collisional quenching is maximized to approximate to the gas kinetic collision frequency and so becomes invariant as every collision relaxes the molecule either rotationally, vibrationally, or electronically. In atmospheric pressure flames, the time between collisions is of the order of 1−5 ns. Nevertheless, the significant concentration levels of OH offset the resulting low fluorescence efficiency that results in such flames using this mode. Fluorescence efficiency is approximately $(\tau k_q[M])^{-1}$ or about $(3 \times 10^9\tau)^{-1}$ at 2000 K. τ is the radiative lifetime, and for OH(A,$v = 1$), 736 ns, k_q is the overall rate of quenching, and [M] is the gas density. Consequently, in the present case, the efficiency is about 0.05% and still sufficient for adequate monitoring.

For measurements involving the CH($A^2\Delta-X^2\Pi$) and C_2-($d^3\Pi_g-a^3\Pi_u$) transitions, a similar mode could not be used as these have corresponding $v' = 0$ lifetimes of about 537 and 100 ns, respectively, and concentrations several orders of magnitude below those of OH. For these, a laser saturation method had to be used to gain the independence from collisional quenching. A Quanta Ray Nd.Yag pumped dye laser with doubling crystals and a high finesse Etalon narrowed the laser line width to be compatible with the flame Doppler linewidths. For CH, the close lying $R_{1cd}(7)$ and $R_{2dc}(7)$ transitions at 426.776 and 426.780 nm of the ($A^2\Delta-X^2\Pi$), (0,0) band system were simultaneously pumped saturating the $N' = 8$ levels of the two sub-states.[70,71] Such rotational levels exhibit maximum population at these temperatures, and transition probabilities are large. Q-branch transitions from $N' = 8$ of this (0,0) band at 430.9 nm were monitored. The bandpass undoubtedly includes emission from adjacent relaxed rotational states. However, these are not locked in saturation by the laser and, being subject to normal quenching, will be severely attenuated. As a result, the signal will result predominantly from only the pumped levels.

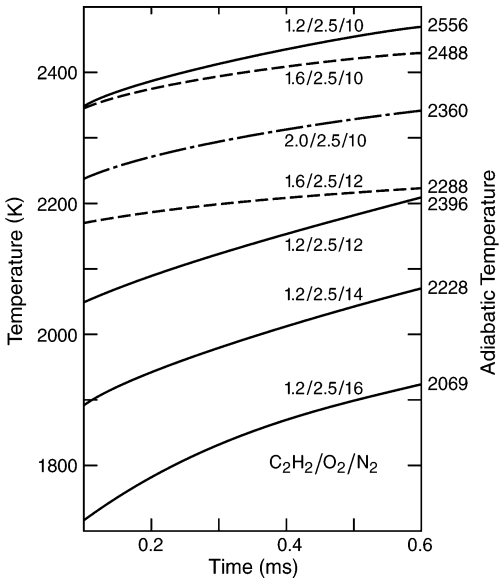

Figure 1. Measured flame temperatures as a function of downstream time in the early burned gas region of the $C_2H_2/O_2/N_2$ flames together with their calculated equilibrium adiabatic temperatures. The unburned gas volume ratios of $C_2H_2/O_2/N_2$ are indicated for the seven flames on their respective curves.

In the case of C_2, the smaller rotational constant produces a less open rotational band structure, making selective laser pumping of a single vibronic state difficult with normal dye laser linewidths. The peak C_2 concentrations at flame temperatures are in the region of $N = 15-20$, and an optimum arrangement was found in pumping the ($d^3\Pi_g-a^3\Pi_u$), (0,0), P(11−16) levels at 516.503 nm. Detection was in the corresponding P branches of the (0,1) transition in the region of 563.5 nm.[72] Although several transitions are saturated simultaneously, this should not detract from the general quality of the measure.

In both cases using saturated LIF, measurements were made at differing laser energies to ensure that no laser perturbations were occurring. This confirmed that the data did reflect the natural CH and C_2 concentrations that are present. It has been shown that saturated LIF is valid for monitoring C_2 but only for non-sooting equivalence ratios as those used herein.[64] The raw fluorescence intensities of CH and C_2 were converted to relative concentration scales after applying corrections for differing flame temperatures that slightly modify the population of their pumped states.

V. Experimental Results and Preliminary Implications

Temperature and OH, H Measurements. Appropriate portions of the flame temperature profiles close to the reaction zone are indicated in Figure 1, as a function of downstream time for the seven acetylene flames. As seen by the calculated adiabatic temperatures also listed,[73] by a time of 100−600 μs from the reaction zone most of the heat release has already occurred. Moreover, due to radiative losses and stabilizing heat loss to the burner surface, final temperatures will not even reach these adiabatic expectations. At 0.2 ms (200 μs) from the reaction zone, the hottest four flames are well within 5% of their final temperature and the lower more non-equilibrated flames within about 10%. This reflects the extremely rapid chemistry that occurs not only in the reaction zone but also in the narrow pre-heating zone that the gases pass through. At atmospheric pressure, these zones for hydrogen or acetylene

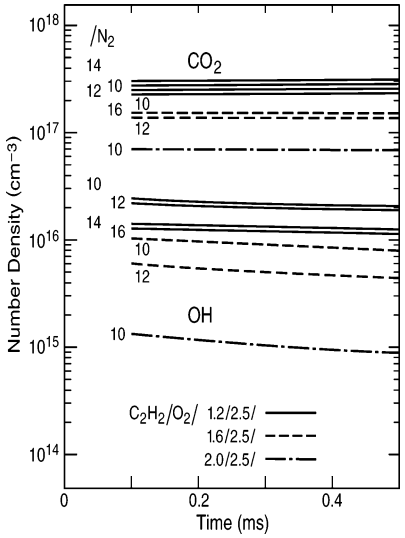

Figure 2. Measured OH absolute concentrations in the seven acetylene flames (seven lower curves) as a function of downstream time. These are used to calculate the CO_2 values (seven upper curves) assuming a partial equilibrium between the hydrogen, oxygen, CO, and CO_2 flame species. The single numbers on the curves identify to which of the seven flames it refers. The four flames with C_2H_2/O_2 volume ratios of 1.2:2.5 ($\phi = 1.2$) have corresponding N_2 ratios of 10, 12, 14, or 16. Similarly, the two 1.6:2.5 ($\phi = 1.6$) flames have N_2 of either 10 or 12, and the single 2.0:2.5 ($\phi = 2.0$) flame has a N_2 ratio of 10.

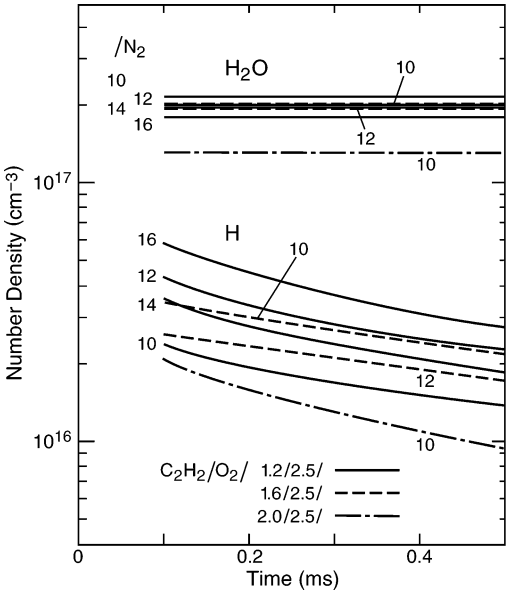

Figure 3. Measured H atom concentrations and calculated H_2O values based on measured OH/H concentrations and assuming a partial equilibrium between the hydrogen, oxygen, CO, and CO_2 flame species. Variations with downstream time in the early burned gas region. The seven flames are labeled as explained in Figure 2.

flames have thicknesses less than 0.1 mm or an approximate time scale of the order of 50 μs.[14]

The corresponding measured concentrations of OH are indicated in Figure 2 for the seven flames as a function of downstream time. Over this brief time range, their concentrations vary but slightly with time. However, in relative magnitudes, a 20-fold variation is observed in the range of concentration levels for the differing equivalence ratios. Moreover, they show an even larger range of non-equilibration. Referring to the OH measurements at 0.2 ms in Figure 2, from the largest concentration shown (1.2/2.5/10) down to the lowest (2/2.5/10), the experimental values are 3.2, 19.3, 44.9, 180.5, 4.1, 6.6, and 1.7 times larger, respectively, than their expected equilibrium values at these measured temperatures.[73] They are all still in the slow process of adjusting from the tremendous energy release and the drastic overshoots of equilibrium that occur in the narrow reaction zone region.

The Na/Li emission comparison method for independently determining H-atom concentrations is well suited to fuel-rich flames.[68] A previous similar application to a series of six fuel-rich $H_2/O_2/N_2$ flames compared such H-atom measurements with those of OH derived by the same LIF method as used here. A test of partial equilibrium between these two radicals using the reaction

$$H_2 + OH = H_2O + H$$

gave a very accurate assessment of its equilibrium constant.[66] In the present case, the same type of plot resulted for these acetylene flames over the full 0.1−4.0 ms range for which these particular measurements were made. This is particularly noteworthy, indicating that similar partial equilibrium concepts for OH and H are valid in these fuel-rich acetylene flames. The corresponding measured values for H-atom concentrations in this early part of the flames are illustrated in Figure 3 and show magnitudes generally above OH in most of these flames and increasingly so with richer equivalence ratios. They show a similar magnitude and trend in relation to the degree of non-equilibration as that indicated above with OH. This agreement not only confirms a partial equilibrium between the H and OH species in these acetylene flames but also lends additional credence to the OH concentration measurements. Baulch et al.[74] have recently published their latest critical evaluation of rate constants pertinent to combustion. As will be seen later, this has been an invaluable asset to the present analysis. Taking the rate constants for the dominant reactions in the H_2/O_2 system and those coupling CO and CO_2, an analysis for the present flames agrees with past assessments. Partial equilibrium between H_2O, H_2, OH, H, O, and O_2 should be almost instantly established and maintained (<10 μs), forming a radical pool in the burned gases. The experimental data herein confirm this for H and OH. However, due to the very low levels of O and O_2 in the fuel richest flame, whether this assumption remains rigorous for these cases, or whether the hydrocarbon radical chemistry can perturb the pool in this regard is an interesting question that has been examined already in the literature.[75−80] The general consensus is that the presence of the hydrocarbon tempers slightly the magnitudes of the radical overshoots in the H_2/O_2 cycle but leaves the pool intact with the proviso that O and O_2 should not be too small.

Moreover, as now well established, the formation of CO_2 from CO can be a rate-limited step certainly in the richer flames. However, in the $\phi = 1.6$ and 2.0 flames at their temperatures in this study, most of the carbon remains as CO even to equilibrium. Consequently, the actual concentrations of CO may remain slightly in excess of their partial equilibrium values in only the leaner flames due to this limitation. If a partial equilibrium is assumed, this permits to a sufficiently good approximation the iterative calculation of the concentrations of the H_2O, CO_2, CO, H_2, O_2, and O species solely from temperature, the experimental OH and H values, and chemical thermodynamic data.[81] So calculated, their concentration profiles as a function of time are illustrated in Figures 2−5. As indicated, even though the partial equilibrium values for CO_2 and CO indicated in Figures 2 and 4, respectively, may be slightly approximate, this has not affected the present analysis to any degree.

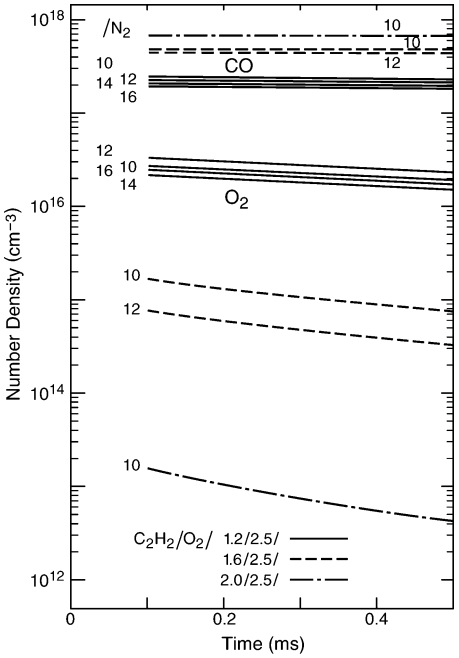

Figure 4. Calculated CO and O_2 concentrations as a function of downstream time based on measured OH/H concentrations and assuming a partial equilibrium between the hydrogen, oxygen, CO, and CO_2 flame species. The seven flames are labeled as explained in Figure 2.

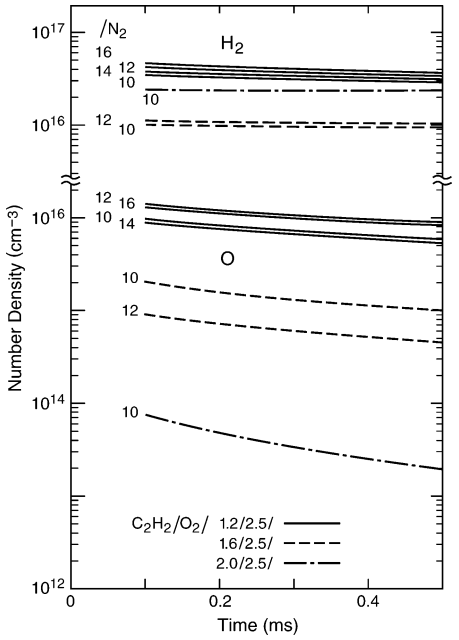

Figure 5. Calculated H_2 and O concentrations as a function of downstream time based on measured OH/H concentrations and assuming a partial equilibrium between the hydrogen, oxygen, CO, and CO_2 flame species. The seven flames are labeled as explained in Figure 2.

In addition, in these fuel-rich flames the HO_2 and NO species are insignificant in these regions and can be ignored. Other than N_2, it is H_2O, CO_2, and CO that are the major burned gas species. H_2 ranks slightly below these, indicating above equilibrium values for $\phi = 1.2$ flames, but being depressed below equilibrium in the richer flames. O and O_2 show the most interesting behavior. As seen in Figures 4 and 5, as expected these tend to be a reflection of each other, showing similar trends and magnitudes. They also illustrate the largest nonequilibrium variations that span up to 4 orders of magnitude, which is close to being the square in magnitude of those noted above with

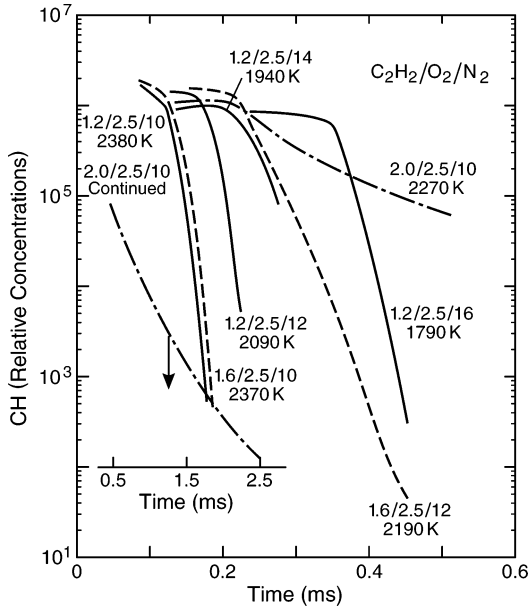

Figure 6. Measured relative concentrations of CH radicals as a function of downstream time in the early burned gases of the seven acetylene flames together with their temperatures at 0.2 ms. Curves are labeled by their individual unburned $C_2H_2/O_2/N_2$ flame ratios.

OH and H. In addition, in the richest flame studied, their concentrations are very small.

Returning to the flame temperatures of Figure 1, a comparison between the premixed unburned input O_2 values and those still existing at 0.2 ms indicates rather surprising results. Already, in the $\phi = 1.2$ flames, 95% of the O_2 has been consumed, and more than 99.8% for $\phi = 1.6$, it having decayed to as low as 3 ppmv in the richest flame. Even so, chemistry is still occurring with significant possible consequences. Indeed, what can be deduced even before looking at the CH and C_2 data are several conclusions for these burned gas regions.

The basic flame species of H_2O, CO_2, CO, H_2, OH, H, O_2, and O are dominant, and any persisting fuel and hydrocarbon radicals will necessarily play a secondary role in these burned gas regions.

The C_2H_2 in the original fuel no longer exists. CO_2, CO, and carbon-bearing radical fragments have replaced it. Any C_2H_2 observed must have been reformulated. CH and C_2 radical concentrations are small in the burned gases because the total concentration of all of the carbon-bearing fragments is small.

From the point of view solely of energy release, the combustion is essentially over. In the present seven flames, at 0.2 ms downstream the $\phi = 1.2-2.0$ flame gas compositions are 82−62% N_2, 11−24% ($CO + CO_2$), 7−4% H_2O, 1.1−0.3% H_2, 0.6−0.5% H, 0.8%-370 ppmv OH, 0.8%-3.4 ppmv O_2, and 0.3%-15 ppmv O, respectively. Even so, this is the region where the major remaining hydrocarbon fragments such as CH and C_2 are observed with concentrations more on a <0.1% (<1000 ppmv) scale.

Despite these aspects, the low levels of hydrocarbon fragments that remain still are of intrinsic interest. They are the basis for spectral emissions, for NO_x and soot formation, ionization, and for diamond flame deposition.

Relative Concentration Profiles for CH and C_2. The seven profiles of the measured relative concentrations of CH and C_2 in this series of flames are illustrated in Figures 6 and 7. Although not calibrated here absolutely, they are expected to reflect ppmv concentration scales. Closer inspection indicates that these two figures contain numerous interesting aspects. The

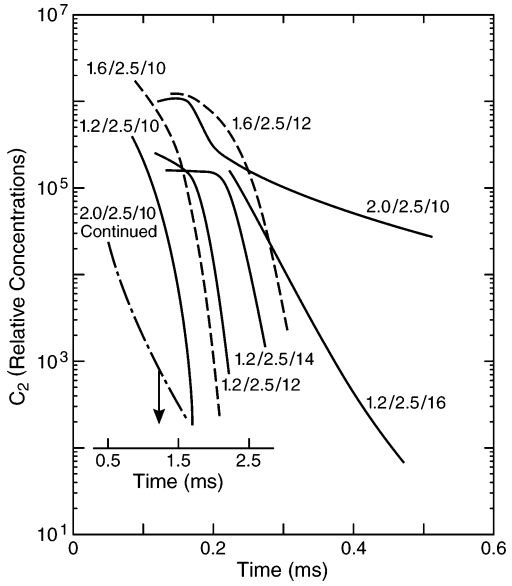

Figure 7. Corresponding measurements to the previous figure but for the relative concentrations of C_2 in the early burned gases of the seven acetylene flames.

most immediate and striking visual factor is that the profiles for the two species show very similar trends. Without looking at the labeling, it is hard to say which is which. However, closer examination does show that CH is slightly displaced to longer times. Also, in the four $\phi = 1.2$ flames, profiles are lengthened by decreased temperatures, an effect also seen in the two $\phi =$ 1.6 flames. Lengthening also correlates with fuel richness. For CH, this reflects the lengthening reported previously in low-pressure flames.[24−26]

Another notable component is the fact that, at 0.1 ms, the closest point to the flat reaction zone where measurements could be made, the initial concentrations for CH start out at similar concentration levels and also with C_2 but to a lesser exactness. On calculating the total carbon content of a unit volume of the burned gases for each of these seven flames, a total variation of only a factor of 2 is noted. Consequently, the CH data imply that it forms from the total carbon in roughly a constant yield fraction. In addition, a very pronounced difference is seen in their profile decay shapes between the 1.2/2.5/10 ($C_2H_2/O_2/N_2$) and richer 2.0/2.5/10 flames, which only differ in temperature by 100 K. Whereas the two radicals rapidly decay within 0.1 ms in the former flame, data extend to 1.5 or 2.5 ms in the richest flame.

Such similar profile shapes for CH and C_2 have been illustrated before in low-pressure flames, not only for C_2H_2/O_2[18,20,23] but also with CH_4, C_2H_6, and C_2H_4.[10,23] However, although noticeable, the fact was not commented upon. Moreover, it is apparent also in two atmospheric pressure studies. Ni et al.[82] monitored their two-dimensional LIF distributions on a pipe burner with a slightly fuel-rich premixed LPG/air and an iso-octane/air flame. They reported a similar pattern for the two radicals in each flame, but the pattern differed from flame to flame. Mercier et al.[64] examined two laminar CH_4/air diffusion flames on a three-slot burner using LIF and cavity ring-down methods to monitor C_2. A comparison with their earlier work with CH indicated a good spatial correlation between the two sets of profiles. Consequently, the present observation is supported by previous work. This is the first study though that shows such a consistent pattern of behavior for these two species over a wide range of equivalence ratios with such differing flame species compositions. Coupling this to the previous data, such a close coincidence of concentration profile patterns cannot be by chance. These cover a range of pressures, fuels, and burning methods, so there seems to be little doubt that somehow the two radicals are connected by the very general nature of combustion.

VI. Chemical Kinetic Implications

The Chemical Kinetics of CH and C_2. Fortunately, a recent very comprehensive and valuable critical evaluation of kinetic data for combustion modeling has been published.[74] Armed with this, together with previous extensive kinetic models such as GRI-Mech 3.0[8] and even more recently published data, it was decided to dissect the hundreds of reactions that can occur in acetylene flames. However, emphasis was concentrated only on this first 0.1−0.5 ms (100−500 μs) time period of the burned gases, which simplified this daunting task somewhat.

As already shown by kinetic modelers, time is the dominant controlling parameter for ranking the relative importance of reactions especially under the present constraint. Combustion chemistry is remarkably rapid, and dominant controlling reactions occur on sub-microsecond time scales. As a result, it is immediately apparent at 50−100 μs from the reaction zone that these acetylene flames are no longer that. They have already changed and been reformulated. Now they are essentially hydrogen flames containing substantial CO and CO_2, together with a myriad of smaller amounts of a large number of hydrocarbon species. As seen in Figures 2−4 at atmospheric pressure, concentrations of the major species of H_2O, CO, and CO_2 are on 10^{17} molecule cm^{-3} (percentage) scales. In addition, as also seen in Figures 2, 3, and 5, because the flames are fuel rich they contain H_2, H, and OH concentrations on a 10^{16} molecule cm^{-3} (0.3%) scale. This immediately implies that any hydrocarbon fragment that has a reaction with H_2, H, or OH and a rate constant at 2000 K that reflects a gas kinetic unit collision efficiency will automatically have a reactive half-life of about 0.2 μs and be important. A reaction with either H_2O, CO, or CO_2 can be much less efficient yet still retain a dominant role. Competing with these, O_2 and O have a more difficult task as their reactivities toward hydrocarbons generally are reduced below those of H and OH. Also, as seen in Figures 4 and 5, although O_2 and O concentrations start out at a 10^{16} molecule cm^{-3} level in $\phi = 1.2$ flames, these rapidly decrease with increasing equivalence ratio to the extremely low values at $\phi = 2.0$ of 10^{13} molecule cm^{-3} (3.4 and 15 ppmv, respectively, for O_2 and O). Moreover, C_2H_2 and any other fragment hydrocarbon species have already been reduced to levels that generally are on a scale measured in hundreds of ppmv. In other words, in this region where hydrogen/oxygen flame radicals are very important, it will be difficult for any hydrocarbon−hydrocarbon interaction to compete. For example, two hydrocarbon species each with a concentration of 500 ppmv that interact with a rate constant of 1×10^{-10} cm^3 $molecule^{-1}$ s^{-1} will have a reactive half-life of about 5 μs. In other words, although such interactions may have been important in the reaction zone region where the hydrocarbon fuel concentration was high and being consumed, by 100 μs a different regime now exists. This is one controlled by the radical pool of H_2O, H, OH, H_2, O, O_2, together with CO and CO_2. To further prove the point, the reactions invariably quoted in models as coupling C_1 to C_2 hydrocarbon species:

$$CH_3 + CH_3 + M = C_2H_6 + M$$

$$CH_3 + CH_3 = C_2H_5 + H$$

TABLE 1: Currently Recommended Heats of Formation, kJ mol^{-1}

species	ΔH_{298K}^f	ref	species	ΔH_{298K}^f	ref
$C(^3P)$	716.68(±0.44)	83	$CHCO(^2A'')$	176.6(±3)	90
$CH(^2\Pi)$	595.8(±0.6)	84	$CH_2C(^1A)$	410(±10)	91,92
$CHO(^2A')$	43.0(±1.5)	85,86	$C_2H_2(^1\Sigma)$	227.4(±0.8)	83
$CHO^+(^1\Sigma)$	833(±8)	74	$CH_2CO(^1A)$	−47.5(±1.7)	74
$CHOH(^1A)$	109(±4)	87	$C_2O(^3\Sigma)$	381.2(±2.0)	93
$CH_2(a^1A)$	428.8(±1.6)	84	$H(^2S)$	217.998(±0.006)	94
$CH_2(X^3B)$	391.2(±1.6)	84	HCCOH	93.2	74
$CH_2O(^1A)$	−108.7(±0.5)	83	$HCN(^1\Sigma)$	135.2(±8)	74
$CH_2OH(^2A)$	−17.0(±0.7)	84	$HOCO(^2A')$	−195(±10)	95
$CH_3(^2A'')$	146.7(±0.3)	84	$HO_2(^2A'')$	13.0(±1.0)	96,97
$CH_3O(^2\Sigma)$	21.0(±2.1)	84	$H_2(^1\Sigma)$	0	
$CH_3OH(^1A')$	−201.0(±0.6)	83	$H_2O(^1A_1)$	−241.83(±0.04)	94
$CH_4(^1A_1)$	−74.6(±0.3)	83	$N(^4S)$	472.68(±0.4)	74
$CO(^1\Sigma)$	−110.53(±0.17)	83	$NCN(^3\Sigma)$	473(±20)	74
$CO_2(^1\Sigma)$	−393.51(±0.13)	83	$N_2(^1\Sigma)$	0	
$C_2(a^3\Pi)$	829.6(±2)	88	$O(^3P)$	249.18(±0.10)	94
$C_2(X^1\Sigma)$	822.3(±2)	88	$OH(^2\Pi)$	37.3(±0.3)	84
$C_2H(^2\Sigma^+)$	566.6(±0.8)	89	$O_2(^3\Sigma)$	0	

are relatively slow in this specific regime.[74] These reactions each require CH_3 concentrations of 6.5×10^{16} molecule cm^{-3} (1.8%) for reactive half-life values of even 10 μs. As a result, any reaction between two hydrocarbon fragments is relegated to a slower secondary level in this region.

Because of such implications, it was decided to examine in detail the flame chemistry of the numerous hydrocarbon species in these flames. Emphasis has centered on this time region and especially around 0.2 ms from the reaction zone. The reactant species are H_2O, CO, CO_2, H_2, H, OH, O_2, and O. The hydrocarbon species included are C, CH, CH_2, CH_3, CH_4, CHO, CHOH, CH_2O, CH_3O, C_2, C_2H, C_2H_2, CHCO, CH_2CO, CH_2OH, CH_3OH, and C_2O. Previously, these all have been monitored in flames with the exception of CHOH, the isomeric form of formaldehyde. Every possible algebraic interaction between these two sets of potential reactants has been assessed. By taking or estimating their rate constants, a list of the most probable formation and loss reactions for each hydrocarbon species has been established. Because only efficient and fast reactions are plausible as being significant in this time-constrained region, certain criteria exist that simplify the reaction database. So-called four-center reactions were discarded, as were any complex interactions that require multiple bond breaking and forming. Also, the magnitudes of adverse enthalpies automatically eliminated some reactions due to their necessarily reduced efficiencies. The enthalpy values used in this exercise are listed in Table 1. These are regarded as the most reliable current set. As a result, an initial list of several hundred reactions was cut to about 150 that might be playing important roles. Additionally, in this rigorous process, several new potential reaction channels have become apparent for some species that have not been considered previously. Moreover, it became clear for this analysis that it was not critical to have an all-inclusive list.

Table 2 for CH lists all its formation and loss reactions using the above criteria. It shows the complex network of reactions that can produce it from the multitude of other hydrocarbon radicals and similarly destroy it to produce a further myriad of new hydrocarbon radicals. Although rate constant data still are required for some of its formation channels, its rates of removal are now quite well defined. For illustrative purposes, the relative rates of these reactions are also listed in the table at 0.2 ms downstream for the three different equivalence ratios of the flames with O_2/N_2 ratios of 2.5/10. This follows an approach used by Burgess and Langley[80] to approximately convey the relative importance of reactions. It has been called the characteristic reaction time. This assumes an excess of one reactant and gives the time required for the reaction to reduce the concentration of the minor reactant by a factor of 1/e, a half-life $\tau_{1/e} = (k[M])^{-1}$. It is particularly useful for easily ranking the importance of removal channels, but requires the additional concentrations of the individual hydrocarbon fragments to examine the dominant formation pathways. Coupling the rate data of Table 2 with the flame concentrations, the rate of loss of CH can be calculated. This implies an average collisional removal half-life at 0.2 ms in the seven flames studied, $(\sum_i(k_i[M_i])^{-1}$, of about 0.05−0.12 μs. Consequently, the CH flame profile observed in Figure 6, which is on a hundreds of microsecond time-scale, is a reflection of a very dynamic kinetic system. It is not the simple decaying loss profile of a species initially made and now being destroyed. It is a profile of a species that is made and destroyed thousands of times during the recording. Moreover, throughout this time region, the flame temperatures and the basic flame hydrogen/oxygen and CO/CO_2 concentration levels are not markedly changing. Nevertheless, the CH profiles modify quite drastically by over 3 orders of magnitude. Some additional factor obviously is controlling its rate of formation, and as this ceases CH disappears instantly. These thoughts also tie back into the previously mentioned paper of Chou and Dean.[65] As already noted, they perturbed a methane-based flame with a pulsed 193 nm laser and then monitored the decay of the newly created CH radical. It had a half-life of about 5 μs. This in fact now appears to be far too long. In other words, the laser must have affected the whole hydrocarbon fragment distribution for it to take this length of time to readjust.

Table 3 lists corresponding data for C_2. Fewer reactions occur for this, and rate data are sparse. It is apparent that formation necessarily is solely from C_2H. The data are more uncertain and largely estimated. Nevertheless, there is a sufficient foundation to indicate that this is also involved in a very dynamic kinetic cycle of formation and loss. Approximate estimates of the collisional removal half-lives at 0.2 ms in these seven flames fall in the range of 0.15−0.56 μs, still remarkably fast. As shown by the data in Table 3, the low-lying $C_2(a^3\Pi_g)$ state is necessarily equilibrated with its $X^1\Sigma_g^+$ ground state due to their efficient coupling and so are indistinguishable in flames.

What is obvious is that the CH and C_2 flame radicals are very different in chemical nature. Initial thoughts that the two species may be intimately related by direct interconversion or that their production and loss mechanisms were similar are now seen to be naïve. C_2 has to be produced predominantly from

TABLE 2: Appropriate Rate Constants and Approximate Reaction Lifetimes for CH Formation and Removal in These Flames

reaction	ΔH_{298K} kJ mol^{-1}	k cm^3 molecule^{-1} s^{-1}	T, K range	k_{2000K}	$\tau_{1/e}$ ($N_2 = 10$), μs[a] $\phi = 1.2$	1.6	2.0	dominant channels	ref/comments
formation reactions:									
$C + H_2 = CH + H$	+97	6.6(−10) exp(−11 700/T)	1525−2540	1.9(−12)	6.2	21	11		74
$C + OH = CH + O$	+91	4(−10) exp(−10 950/T)	1500−2500	1.7(−12)	10	25	259		estimate, 1 of 2 channels
$CH_2 + H = CH + H_2$	−13	2(−10)	298−3000	2.0(−10)	0.3	0.2	0.3	*	74
$CH_2 + OH = CH + H_2O$	−75	1.9(−17)$T^{2.0}$ exp(−1510/T)	1000−2500	3.6(−11)	0.7	1.8	17		8, 1 of 4 channels
$CH_2 + O = CH + OH$	−7	8(−11)	1000−2500	8(−11)	1.5	7.8	250		estimate, 8,74, 1 of 2 channels
$CHOH + H = CH + H_2O$	+27	1(−11)	1000−2500	1(−11)	5.1	3.3	6.3		estimate, 1 of 3 channels
$C_2H + O = CH + CO$	−331	2(−11)	1000−2500	2(−11)	6.0	31	1000		estimate, 74, 1 of 4 channels
$CHCO + O = CH + CO_2$	−223	4.9(−11) exp(−560/T)	298−1000	3.7(−11)	3.1	16	522		74, 1 of 3 channels
$C_2O + H = CH + CO$	−114	8(−11)	1000−2500	8(−11)	0.6	0.4	0.8	*	31
loss reactions:									
$CH + N_2 = HCN + N$[b]	+12[d]	6.0(−12) exp(−11 060/T)	1000−4000	2.4(−14)	7.7	8.5	11		74, $k(b + c)$
$= NCN + H$[c]	+95								d, spin forbidden
$CH + CO_2 = CHO + CO$	−270	1.1(−16)$T^{1.5}$ exp(360/T)	298−3500	1.2(−11)	0.2	0.4	1.0	*	74
$CH + CO = C_2O + H$	+114	3.1(−13)	2500−3500	3.1(−13)	13	6.5	4.5		74
$CH + H_2O = CHOH + H$[e]	−27	7.6(−8)$T^{-1.42}$	298−1000	1.6(−12)	3.7	3.9	5.9		74, $k(e + f)$
$= CH_2 + OH$[f]	+75								
$CH + H_2 = CH_2 + H$	+13	2.9(−10) exp(−1670/T)	200−1000	1.3(−10)	0.2	0.7	0.3	*	74
$CH + H = C + H_2$	−97	2.0(−10)	1500−2500	2.0(−10)	0.3	0.2	0.3	*	74
$CH + OH = CHO + H$[g]	−372	5(−11)	1000−2500	5(−11)	0.8	2.0	17		$k(g + h + i)$ estimate, 8
$= C + H_2O$[h]	−158								
$= CH_2 + O$[i]	+7								
$CH + O_2 = CHO + O$	−304	1.4(−10)	2200−3500	1.4(−10)	0.3	5.3	649		74
$CH + O = CO + H$	−738	6.6(−11)	298−2000	6.6(−11)	1.8	9.5	303		74
$= C + OH$	−91	2.5(−11) exp(−2380/T)?	1600−2000	7.6(−12)?	13	68	2283		74
$= CHO^+ + e^-$	−12	4.2(−13) exp(−850/T)	298−2500	2.7(−13)	410	2130	69 250		74

[a] Illustrative reaction half-life ($\tau_{1/e}$) values in μs at 0.2 ms downstream in three of the $C_2H_2/O_2/N_2$ flames (1.2/2.5/10, 1.6/2.5/10, 2.0/2.5/10) to convey relative reaction importance. The average total collisional removal half-life for CH is 50−120 ns at 0.2 ms in the seven acetylene flames studied.

TABLE 3: Appropriate Rate Constants and Approximate Reaction Lifetimes for C_2 Formation and Removal in These Flames

reaction	ΔH_{298K} kJ mol^{-1}	k cm^3 molecule^{-1} s^{-1}	T, K range	k_{2000K}	$\tau_{1/e}$ ($N_2 = 10$), μs[a] $\phi = 1.2$	1.6	2.0	dominant channels	ref/comments
formation reactions:									
$C_2H + H = C_2 + H_2$	+38	1.0(−10) exp(−8767/T)	1500−2500	1.2(−12)	20	13	30		74, theory, 98
$C_2H + OH = C_2 + H_2O$	−23	6.6(−17)$T^{2.0}$ exp(−4025/T)	1000−2500	3.5(−11)	0.6	1.5	14	*	9, 1 of 3 channels
$C_2H + O = C_2 + OH$	+44	2(−11)	1000−2500	2.0(−11)	6	31	1000		estimate, 1 of 4 channels
loss reactions:									
$C_2(a) + CO_2 = C_2O + CO$	−165	?	1000−2500	5(−12)	0.9	1.6	3.6	*?	estimate
$C_2 + H_2O = C_2H + OH$	+23	?	1000−2500	5(−12)	0.9	1.0	1.5	*?	estimate, theory, 99
$C_2 + H_2 = C_2H + H$	−38	1.1(−10) exp(−4000/T)	2580−4650	1.5(−11)	1.5	4.9	2.2	*	74, theory, 98
$C_2 + OH = CHO + C$	−100	?		1(−11)	4.2	10	83		estimate
$= C_2O + H$	−260	2(−11)?	1000−2500	2(−11)	2.1	5.0	42		9, estimate
$= C_2H + O$	−44	?		1(−11)	4.2	10	83		estimate
$C_2 + O_2 = C_2O + O$	−192	2.8(−10) exp(−4070/T)	2750−3950	3.7(−11)	0.8	15	1950		74
$C_2 + O = CO + C$	−465	1.3(−9) exp(−6250/T)	2750−3950	5.7(−11)	1.3	6.7	240		100
$C_2(a) + M = C_2(X) + M$	−7	2.7(−11)	300	7(−11)	0.2	0.3	0.8		74, M = H,OH,O,O_2

[a] Reaction half-life as explained in the footnote of Table 2. The average total collisional removal half-life for C_2 is approximately 0.15−0.56 μs at 0.2 ms in the seven acetylene flames.

C_2H, and CH predominantly from CH_2. Their removal channels are many and varied. Even so, they obviously are indirectly connected.

The Chemical Kinetics of the Other Hydrocarbon Species. Lists similar to those of Tables 2 and 3 for CH and C_2 have been created for all of the hydrocarbon species included in this analysis. Because interest lies only with the dominant reactions in this roughly 100−500 μs time period and due to the large number, only the most efficient are listed for illustration in Table 4. Even so, this is a significant tabulation of interconnected reactions. It reflects the richness that is organic chemistry.

Even a scant perusal of Table 4 indicates two keywords, "estimate" and "channels", implying significant uncertainties. This is still the bane of the kinetic modeler in endeavoring to examine the chemistry in finer detail. Fortunately, it has not been a limiting factor for the present analysis that is not looking for a quantitative exact fit to data but rather a general explanation. From Table 4, it is obvious that if one of the major species such as H_2O, CO, or CO_2 has potential reaction channels, these do not necessarily need to be efficient due to their large driving force concentrations. Because of this, they can have significant adverse reaction enthalpies yet remain important.

TABLE 4: Fast Reactions That Couple Hydrocarbon Radicals One to Another in the Early Burned Gases of These Acetylene Flames

hydrocarbon species		dominant reactions	ΔH_{298K} kJ mol^{-1}	k_{2000K} cm^3 molecule^{-1} s^{-1}	reactant radical lifetime $\tau_{1/e}$ (N_2 = 10), μs[a] ϕ = 1.2	1.6	2.0	fast channels	ref/comments
C	formation	$CH + H = C + H_2$	−97	2(−10)	0.3	0.2	0.3	*	74
		$C_2 + OH = C + CHO$	−100	1 (−11)	4.2	10	83		estimate, 1 of 3 channels
		$C_2 + O = C + CO$	−465	5.7(−11)	1.3	6.7	240		100
		$C_2H + O = C + CHO$	−56	2 (−11)?	6.0	31	1000		74, estimate, 1 of 4 channels
		$C_2O + O = C + CO_2$	−307	4 (−11)?	3.0	16	500		estimate, 1 of 2 channels
	loss	$C + CO_2 = CO(a) + CO$	+36	?					role if $k \approx 7(-12)$
		$C + H_2O = CHO + H$	−214	5 (−12)	0.6	0.6	1.1	*	101, estimate
		$C + H_2 = CH + H$	+97	1.9(−12)	6.2	21	11		74
		$C + OH = CO + H$	−647	8 (−11)	0.5	1.3	10	*	8,31, estimate, 1 of 2 channels
		$C + O_2 = CO + O$	−578	9.4(−11)	0.4	7.7	950		74
CH	formation	$CH_2 + H = CH + H_2$	−13	2.0(−10)	0.3	0.2	0.3	*	74
		$CH_2 + OH = CH + H_2O$	−75	3.6(−11)	0.7	1.8	17		8, 1 of 4 channels
		$C_2O + H = CH + CO$	−114	8 (−11)	0.6	0.4	0.8	*	31
	loss	$CH + CO_2 = CHO + CO$	−270	1.2(−11)	0.2	0.4	1.0	*	74
		$CH + H_2 = CH_2 + H$	+13	1.3(−10)	0.2	0.7	0.3	*	74
		$CH + H = C + H_2$	−97	2.0(−10)	0.3	0.2	0.3	*	74
		$CH + O_2 = CHO + O$	−304	1.4(−10)	0.3	5.3	649		74
CH_2	formation	$CH + H_2 = CH_2 + H$	+13	1.3(−10)	0.2	0.7	0.3	*	74
		$CH_3 + H = {}^1CH_2 + H_2$	+64	5.5(−12)	5.5	3.6	7.7		74
		$CH_2OH + H = {}^1CH_2 + H_2O$	−14	2.2(−11)	2.3	1.5	2.9		8, 1 of 5 channels
		$CHCO + H = CH_2 + CO$	−114	2.2(−10)	0.2	0.2	0.3	*	74, 1 of 3 channels
		$CH_3 + OH = {}^1CH_2 + H_2O$	+3	2.8(−11)	1.6	3.9	32		102,103, 1 of 4 channels
	loss	${}^1CH_2 + H_2O = CH_3 + OH$	−3	1 (−10)	1.4	1.5	2.4		$\tau_{(CH_2total)}$, 102,104, 1 of 2 channels
		$CH_2 + H = CH + H_2$	−13	2 (−10)	0.3	0.2	0.3	*	74
		$CH_2 + OH = CH + H_2O$	−75	3.6(−11)	0.7	1.8	17		8, 3 of 4 channels
		$= CH_3 + O$	−33	?					branching uncertain
		$= CH_2O + H$	−319	2.6(−11)	1.6	3.8	32		103
		$CH_2 + O = CH + OH$	−7	8 (−11)	1.5	7.8	250		8,74, estimate
		$= CHO + H$	−379	1 (−10)	1.2	6.3	910		branching uncertain
		${}^1CH_2 + N_2 = {}^3CH_2 + N_2$	−38	1.8(−11)	0.02	0.03	0.03	*	74, (${}^1CH_2$) = 3%(${}^3CH_2$)
		$+ H_2O = {}^3CH_2 + H_2O$	−38	2.7(−11)	0.17	0.17	0.28		thermally equilibrated
		$+ CO_2 = {}^3CH_2 + CO_2$	−38	2.2(−11)	0.16	0.28	0.65		
CH_3	formation	$CH_3O + CO = CH_3 + CO_2$	−157	1.3(−12)	1.8	0.9	0.7	*	105, 1 of 2 channels
		${}^1CH_2 + H_2O = CH_3 + OH$	−3	1 (−10)	1.4	1.5	2.4	*	$\tau_{(CH_2total)}$, 102,104, 1 of 2 channels
		$CH_4 + H = CH_3 + H_2$	+3	1.6(−11)	1.4	0.9	2.1	*	74
		$CH_2OH + H = CH_3 + OH$	−17	6.0(−11)	0.8	0.5	1.0	*	8, 1 of 5 channels
		$CH_3O + H = CH_3 + OH$	−55	2.3(−11)	2.2	1.4	2.7	*	74, 1 of 4 channels
		$CH_2CO + H = CH_3 + CO$	−134	1.7(−11)	2.3	1.5	3.1	*	74, 1 of 3 channels
		$CH_4 + OH = CH_3 + H_2O$	−58	1.8(−11)	1.4	3.4	32		74, 1 of 2 channels
	loss	$CH_3 + H_2O = CH_3OH + H$	+112	4.8(−13)	3.2	3.5	7.3	*	estimate, 1 of 2 channels
		$CH_3 + H = {}^1CH_2 + H_2$	+64	5.5(−12)	5.5	3.6	7.7	*	74
		$CH_3 + OH = {}^1CH_2 + H_2O$	+3	2.8(−11)	1.6	3.9	32		102,103, 1 of 4 channels
		$CH_3 + O = CH_2O + H$	−287	1.8(−10)	0.7	3.4	108	*	74, CH_2O, CO products
		$= CH_2 + OH$	+33	?					CH_2 minor?, 106
CH_4	formation	$CH_3 + H_2O = CH_4 + OH$	+58	8.2(−14)	18	20	41		74, 1 of 2 channels
		$CH_3 + H_2 = CH_4 + H$	−3	7.6(−13)	17	59	30		74
		$CH_3O + H = CH_4 + O$	−64	8 (−12)?	6.4	4.2	7.9	*	estimate, 1 of 4 channels
		$CH_3OH + H = CH_4 + OH$	−54	5 (−12)?	10	6.7	13	*	estimate, 1 of 4 channels
	loss	$CH_4 + H = CH_3 + H_2$	+3	1.6(−11)	1.4	0.9	2.1	*	74
		$CH_4 + OH = CH_3 + H_2O$	−58	1.8(−11)	1.4	3.4	32		74, 1 of 2 channels
		$CH_4 + O = CH_3 + OH$	+9	2.5(−11)	2.4	13	480		74, 1 of 2 channels
CHO	formation	$CH + CO_2 = CHO + CO$	−270	1.2(−11)	0.2	0.4	1.0	*	74
		$CH_2OH + CO = CHO + CH_2O$	+62	?					If $A \geq 2(-11)$, 1 of 2 channels
		$CH_3O + CO = CHO + CH_2O$	+24	8 (−13)?	4.9	2.5	1.7		estimate, 1 of 2 channels
		$C + H_2O = CHO + H$	−214	?				?	if $k \approx 1(-12)$, 1 of 2 channels
		$CH_2O + H = CHO + H_2$	−66	9.6(−11)	0.4	0.2	0.5	*	74
		$CH + OH = CHO + H$	−372	5 (−11)	0.8	2.0	17		8, 1 of 3 channels
		$CH_2O + OH = CHO + H_2O$	−127	2.0(−11)	2.1	4.9	41		74, 107
	loss	$CHO + M = CO + H + M$	+64	1.3(−12)	0.1	0.1	0.2	*	74
		$CHO + H = CO + H_2$	−372	1.5(−10)	0.3	0.2	0.4	*	74
		$CHO + OH = CO + H_2O$	−433	1.8(−10)	0.2	0.6	4.6		74, 1 of 2 channels

TABLE 4: (Continued)

hydrocarbon species		dominant reactions	ΔH_{298K} kJ mol^{-1}	k_{2000K} cm^3 molecule^{-1} s^{-1}	reactant radical lifetime $\tau_{1/e}$ (N_2 = 10), μs[a] ϕ = 1.2	1.6	2.0	fast channels	ref/comments
CHOH	formation	$CH + H_2O = CHOH + H$	−27	1.6(−12)	3.7	3.9	5.9	*	74, 1 of 2 channels
		$CH_2OH + H = CHOH + H_2$	−92	3 (−11)?	1.7	1.1	2.1	*?	74, estimate, 1 of 5 channels
		$CH_2 + OH = CHOH + H$	−102	3 (−11)	1.4	3.3	28		estimate, 1 of 4 channels
		$CH_2OH + OH = CHOH + H_2O$	−153	3 (−11)	1.4	3.3	28		estimate, 1 of 3 channels
		$CHCO + OH = CHOH + CO$	−215	4 (−11)?	1.0	2.5	21		estimate, 1 of 3 channels
	loss	$CHOH + M = CH_2O + M$	−218	5 (−14)?	15	10	10		108,109, 1of 2 channels
		$CHOH + CO = CHO + CHO$	+88	1 (−13)?	13	6.9	5.9		estimate
		$CHOH + H = CHO + H_2$	−284	2 (−11)	2.6	1.7	3.2	*	estimate, 1 of 3 channels
		$CHOH + OH = CHO + H_2O$	−345	2 (−11)	2.1	5.0	42		estimate, 1 of 2 channels
		$CHOH + O_2 = CHO + HO_2$	−53	2 (−11)	2.0	37	4500		estimate
CH_2O	formation	$CH_3O + M = CH_2O + H + M$	+88	1.7(−13)	0.7	0.7	0.8	*	110, 1 of 2 channels
		$CH_2OH + M = CH_2O + H + M$	+126	6.1(−13)	0.4	0.4	0.4	*	74, 1 of 2 channels
		$CH_2OH + H = CH_2O + H_2$	−310	4 (−11)	1.3	0.8	1.6	*	74, 1 of 5 channels
		$CH_3O + H = CH_2O + H_2$	−348	5.4(−11)	0.9	0.6	1.1	*	74, 1 of 4 channels
		$CH_2 + OH = CH_2O + H$	−319	2.6(−11)	1.6	3.8	32		103, 1 of 4 channels
		$CH_2OH + O_2 = CH_2O + HO_2$	−79	4.7(−11)	0.7	14	1720		74
		$CH_3 + O = CH_2O + H$	−287	1.8(−10)	0.7	3.4	108		106, 1 of 2 channels
		$CH_2OH + O = CH_2O + OH$	−304	1.3(−10)	0.9	5.0	157		111, 1 of 2 channels
	loss	$CH_2O + H = CHO + H_2$	−66	9.6(−11)	0.4	0.2	0.5	*	74
		$CH_2O + OH = CHO + H_2O$	−127	2.0(−11)	2.1	4.9	41		74,107
		$CH_2O + O = CHO + OH$	−60	2.6(−11)	3.7	19	654		74
CH_2OH	formation	$CH_3O + H = CH_2OH + H$	−38	1.0(−11)	3.5	2.3	4.8	*	8, 1 of 4 channels
		$CH_3OH + H = CH_2OH + H_2$	−34	2.3(−11)	1.5	1.0	2.1	*	74, 1 of 4 channels
		$CH_3OH + OH = CH_2OH + H_2O$	−95	3.5(−11)	0.8	2.1	19	*	112, 1 of 2 channels
	loss	$CH_2OH + M = CH_2O + H + M$	+126	6.1(−13)	0.4	0.4	0.4	*	74, 1 of 2 channels
		$CH_2OH + CO = CH_2CO + OH$	+117	2 (−13)?	6.3	3.3	3.0		estimate, 1 of 2 channels
		$CH_2OH + H = {}^1CH_2 + H_2O$	−14	2.2(−11)	2.3	1.5	2.9		8, 3 of 5 channels
		$= CH_3 + OH$	−17	6.0(−11)	0.8	0.5	1.0	*	8
		$= CH_2O + H_2$	−310	4.0(−11)	1.3	0.8	1.6	*	74
		$CH_2OH + O_2 = CH_2O + HO_2$	−79	4.7(−11)	0.7	14	1720		74
		$CH_2OH + O = CH_2O + OH$	−304	1.3(−10)	0.9	5.0	157		111, 1 of 2 channels
CH_3O	formation	$CH_3OH + H = CH_3O + H_2$	+4	5.0(−12)	6.9	4.5	9.4	*	74, 1 of 4 channels
		$CH_3OH + OH = CH_3O + H_2O$	−57	3.0(−12)	9.6	25	227	*	112, 1 of 2 channels
	loss	$CH_3O + M = CH_2O + H + M$	+88	1.7(−13)	0.7	0.7	0.8	*	110, 1 of 2 channels
		$CH_3O + CO = CH_3 + CO_2$	−157	1.3(−12)	1.8	0.9	0.7	*	105, 1 of 2 channels
		$CH_3O + H_2 = CH_3OH + H$	−4	2.5(−12)	7.7	26	12		74, estimate
		$CH_3O + H = CH_3 + OH$	−55	2.3(−11)	2.2	1.4	2.7		74
		$= CH_2O + H_2$	−348	5.4(−11)	0.9	0.6	1.1	*	74
		$= CH_2OH + H$	−38	1.0(−11)	3.5	2.3	4.8		8
		$= CH_4 + O$	−64	8 (−12)?	6.4	4.2	7.9		estimate
CH_3OH	formation	$CH_3 + H_2O = CH_3OH + H$	+112	4.8(−13)	3.2	3.5	7.3	*	estimate, 1 of 2 channels
		$CH_3O + H_2O = CH_3OH + OH$	+57	2.0(−13)	8.5	9.2	19		74
		$CH_3O + H_2 = CH_3OH + H$	−4	2.5(−12)	7.7	26	12	*	74
		$CH_3O + OH = CH_3OH + O$	−10	4.5(−12)	5.1	13	121		74, 1 of 3 channels
	loss	$CH_3OH + H = CH_2OH + H_2$	−34	2.3(−11)	1.5	1.0	2.1	*	74, 2 of 4 channels
		$= CH_3O + H_2$	+4	5.0(−12)	6.9	4.5	9.4		74
		$CH_3OH + OH = CH_2OH + H_2O$	−95	3.5(−11)	0.8	2.1	19	*	112
		$= CH_3O + H_2O$	−57	3.0(−12)	9.6	25	227		112
C_2	formation	$C_2H + H = C_2 + H_2$	+38	1.2(−12)	20	13	30		74, theory, 98
		$C_2H + OH = C_2 + H_2O$	−23	3.5(−11)	0.6	1.5	14	*	9, 1 of 3 channels
	loss	$C_2(a) + CO_2 = C_2O + CO$	−165	5 (−12)	0.9	1.6	3.6	*?	estimate
		$C_2 + H_2O = C_2H + OH$	+23	5 (−12)	0.9	1.0	1.5	*?	estimate, theory, 99
		$C_2 + H_2 = C_2H + H$	−38	1.5(−11)	1.5	4.9	2.2	*	74, theory, 98
		$C_2(a) + M = C_2(X) + M$	−7	7 (−11)	0.2	0.3	0.8		74, equilibrated M = H,OH,O,O_2
C_2H	formation	$CHCO + CO = C_2H + CO_2$	+107	1.3(−13)	11	5.7	5.0		estimate
		$C_2 + H_2O = C_2H + OH$	+23	5 (−12)	0.9	1.0	1.5	*?	estimate, theory, 99
		$C_2 + H_2 = C_2H + H$	−38	1.5(−11)	1.5	4.9	2.2	*	74, theory, 98
		$C_2H_2 + H = C_2H + H_2$	+121	2.1(−12)	5.3	3.6	9.8		74
		$C_2 + OH = C_2H + O$	−44	1 (−11)?	4.2	10	83		estimate, 1 of 3 channels
		$C_2H_2 + OH = C_2H + H_2O$	+60	6.9(−13)	21	51	551		113, 1 of 3 channels
	loss	$C_2H + CO_2 = CHCO + CO$	−107	3 (−12)?	1.1	2.1	4.8		estimate
		$C_2H + H_2O = C_2H_2 + OH$	−60	2.1(−11)	0.1	0.1	0.2	*	114
		$C_2H + H_2 = C_2H_2 + H$	−121	1.3(−10)	0.2	0.5	0.2	*	74
		$C_2H + OH = C_2 + H_2O$	−23	3.5(−11)	0.6	1.5	14		9
		$= C_2H_2 + O$	−127	5 (−11)	0.8	2.0	17		estimate
		$= CHCO + H$	−209	3.3(−11)	1.3	3.0	25		8
C_2H_2	formation	$C_2H + H_2O = C_2H_2 + OH$	−60	2.1(−11)	0.1	0.1	0.2	*	114
		$C_2H + H_2 = C_2H_2 + H$	−121	1.3(−10)	0.2	0.5	0.2	*	74
		$C_2H + OH = C_2H_2 + O$	−127	5 (−11)	0.8	2.0	17		estimate, 1 of 3 channels

TABLE 4: (Continued)

hydrocarbon species		dominant reactions	ΔH_{298K} kJ mol^{-1}	k_{2000K} cm^3 molecule^{-1} s^{-1}	reactant radical lifetime $\tau_{1/e}$ ($N_2 = 10$), μs[a] $\phi = 1.2$	1.6	2.0	fast channels	ref/comments
C_2H_2	loss	$C_2H_2 + H = C_2H + H_2$	+121	2.1(−12)	5.3	3.6	9.8	*	74
		$C_2H_2 + OH = C_2H + H_2O$	+60	6.9(−13)	21	51	551		113
		$= CH_2CO + H$	−94	9.6(−13)	30	74	668		113
		$= CHCOH + H$	+47	6.5(−13)	27	66	676		113
		$C_2H_2 + O = CHCO + H$	−82	3.7(−11)	2.3	12	419		74,115, 1 of 2 channels
CHCO	formation	$C_2H + CO_2 = CHCO + CO$	−107	3 (−12)?	1.1	2.1	4.8	*	estimate
		$C_2O + H_2 = CHCO + H$	+13	2 (−11)?	1.5	5.0	2.1	*	estimate
		$CH_2CO + H = CHCO + H_2$	+6	1.1(−11)	3.4	2.2	4.5	*	8, 1 of 3 channels
		$C_2H + OH = CHCO + H$	−209	3.3(−11)	1.3	3.0	25		8, 1 of 3 channels
		$C_2O + OH = CHCO + O$	+7	4 (−11)?	1.0	2.5	21		estimate, 1 of 2 channels
		$C_2H_2 + O = CHCO + H$	−82	3.7(−11)	2.3	12	419		74, 1 of 2 channels
	loss	$CHCO + CO = C_2H + CO_2$	+107	1.3(−13)	11	5.7	5.0		estimate
		$CHCO + H_2O = CH_2CO + OH$	+55	1.5(−12)	1.8	1.9	3.5		estimate
		$CHCO + H_2 = CH_2CO + H$	−6	8 (−12)	3.2	11	4.6		116
		$CHCO + H = CH_2 + CO$	−114	2.2(−10)	0.2	0.2	0.3	*	74, 1 of 3 channels
		$CHCO + OH = CHOH + CO$	−215	4 (−11)?	1.0	2.5	21		estimate
		$= CH_2CO + O$	−12	1 (−11)	4.2	10	83		estimate
		$= C_2O + H_2O$	−75	2 (−11)	2.0	5.2	40		estimate
		$CHCO + O = CH + CO_2$	−223	3.7(−11)	3.1	16	522		74
		$= CHO + CO$	−493	3 (−11)?	4.0	21	670		74, estimate
		$= C_2O + OH$	−7	3 (−11)?	4.0	21	670		74, estimate
CH_2CO	formation	$CH_2OH + CO = CH_2CO + OH$	+117	2 (−13)?	6.3	3.3	3.0	*	estimate, 1 of 2 channels
		$CHCO + H_2O = CH_2CO + OH$	+55	1.5(−12)	1.8	1.9	3.5	*	estimate
		$CHCO + H_2 = CH_2CO + H$	−6	8 (−12)	3.2	11	4.6	*	116
		$C_2H_2 + OH = CH_2CO + H$	−94	9.6(−13)	30	74	668		113, 1 of 3 channels
		$CHCO + OH = CH_2CO + O$	−12	1 (−11)	4.2	10	83		estimate, 1 of 3 channels
	loss	$CH_2CO + H = CH_3 + CO$	−134	1.7(−11)	2.3	1.5	3.1	*	74, 2 of 3 channels
		$= CHCO + H_2$	+6	1.1(−11)	3.4	2.2	4.5	*	8
		$CH_2CO + OH = CH_2OH + CO$	−117	3.3(−12)	13	32	264		74,117
		$= CHCO + H_2O$	−55	2.5(−12)	17	41	340		74,117
C_2O	formation	$C_2(a) + CO_2 = C_2O + CO$	−165	5 (−12)	0.9	1.6	3.6	*?	estimate
		$CH + CO = C_2O + H$	+114	3.1(−13)	13	6.5	4.5	*	74
		$CHCO + H = C_2O + H_2$	−13	4 (−12)	13	8.3	16		estimate, 1 of 3 channels
		$C_2 + OH = C_2O + H$	−260	2 (−11)	2.1	5.0	42		9,74, estimate, 1 of 3 channels
		$CHCO + OH = C_2O + H_2O$	−75	2 (−11)	2.0	5.2	40		estimate, 1 of 3 channels
		$C_2 + O_2 = C_2O + O$	−192	3.7(−11)	0.8	15	1950		74
		$C_2H + O = C_2O + H$	−217	2.5(−11)	4.8	25	800		74, estimate, 1 of 4 channels
		$CHCO + O = C_2O + OH$	−7	3 (−11)?	4.0	21	670		74, estimate, 1 of 3 channels
	loss	$C_2O + H_2O = CHCO + OH$	+75	4 (−13)?	5.0	5.4	10		estimate
		$C_2O + H_2 = CHCO + H$	+13	2 (−11)?	1.5	5.0	2.1	*	estimate
		$C_2O + H = CH + CO$	−114	8 (−11)	0.6	0.4	0.8	*	31
		$C_2O + OH = CHO + CO$	−486	3.3(−11)	1.3	3.0	25		estimate
		$= CHCO + O$	+7	4 (−11)?	1.0	2.5	21		estimate
		$C_2O + O = C + CO_2$	−307	4 (−11)?	3.0	16	500		estimate
		$= CO + CO$	−851	8 (−11)	1.5	7.8	250		31

[a] Reaction half-life as explained in the footnote to Table 2.

Also, in these fuel-rich flames, H-atom reactions are of extreme importance and quite generally are dominant over those of OH. This is relevant because reactions of hydrocarbons with OH are prone to numerous alternate branches that are yet to be fully characterized at flame temperatures. Reactions with O and O_2 are seen to be of lesser importance and are negligible or nonexistent for some species. Their importance is very apparent for $\phi = 1.2$ flames in which their residual levels are still high, but these decrease rapidly to more fuel-rich equivalence ratios. Interestingly, reactions with O and O_2 generally do not produce CO or CO_2 directly as one might expect but rather another hydrocarbon radical. This is not to say that there are not innumerable reactions with O and O_2, but these are not listed because they are much slower and represent a minor flux. Of additional interest in several cases, for CHO, CH_3O, and CH_2-OH, is that thermal dissociation can be an important loss channel and dominate over competing isomerization.

A role for electronic excitation in a reactant is only plausible for C_2, CH_2, and possibly CH radicals. That for C_2 has been mentioned already. With CH_2, the a^1A/X^3B energy splitting is more substantial (38 kJ mol^{-1}). This implies that a thermal distribution of CH_2 at 2000 K will contain about 3% $CH_2(a^1A)$. In this case, the singlet state is of interest due to its greater reactivity. Several papers report monitoring $^1CH_2$ in flames, the most recent being by Schocker et al.,[118] but accurate measurements remain difficult. However, due to the ease of collisional relaxation with many species (even Ar), it would seem unlikely that its formation and loss reactions in flames will be sufficient to perturb its thermal distribution. As a result, the potential importance of reactions depending on $^1CH_2$ will be largely offset by this 30-fold reduction from the total CH_2 population. Any role in flames for the lowest lying $CH(a^4\Sigma^-)$ state still remains uncertain. This is due to the continued difficulty of measuring this metastable state that has an excitation energy of 71.6 kJ

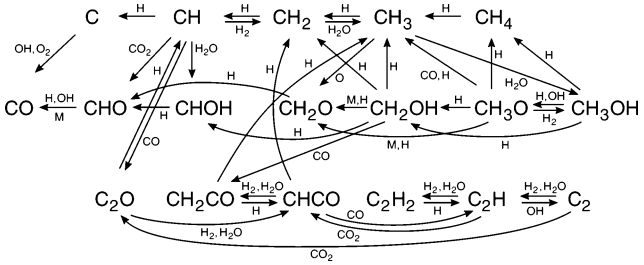

Figure 8. The principal fast reactions of hydrocarbon species and molecules of the hydrogen/oxygen pool together with CO and CO_2 that help to rapidly establish the hydrocarbon radical pool.

mol^{-1}. However, as seen in Table 2, the ground state of CH is so reactive that it will be only in the rarest of cases that CH(a) might be able to compete. As a result, it can probably be safely ignored.

The present analysis differs from such modeling as GRI-Mech 3.0[8] and others by additionally considering C_2, C_2O, and CHOH species. Of these, C_2O may play a greater role than previously has been considered.

What is immediately apparent in Table 4 is that every species has at least one and often several very fast formation and loss reactions that are on or close to sub-microsecond time scales. These are backed by a second layer of slightly slower but also participating reactions. The major reactions that are asterisked in Table 4 are drawn schematically in the reaction network shown in Figure 8. This better illustrates the complex interrelationships and also shows quite clearly the significant kinetic separation between the CH and C_2 species.

What emerges from this analysis is an intriguing mechanism. These hydrocarbon fragments and species form a network of very fast reactions. In this way, they are simply converting from one radical to another and then another and so on. Some, such as CH_2, CH_2O, CH_2OH, CH_3, CH_3O, CH_3OH, CH_4, C_2H, and C_2H_2, have no or only minor direct oxidation channels to CO. Consequently, they constantly interconvert until possibly being removed by oxidation. As may have been expected and is normally seen for species at such concentration levels, they rapidly form various steady-state distributions. However, in addition and more importantly, the majority of these hydrocarbon fragments or molecules also are seen to lose their independence and form a close-knit pool of radicals. As seen in Figure 8, this does not include the C, CH_2O, CHOH, and CHO species. Although in steady states, these four are irreversibly on a direct course of oxidation to CO and lie outside the radical pool, which they cannot join. Such loss reactions from the pool constitute a drain on its overall composition and result from interactions with the remaining levels of oxygen or with OH to produce such species and ultimately CO. These leakage (oxidation) rates out of the pool are largest for near stoichiometric ($\phi = 1.2$) flames due to the still high levels of O_2 and O, which are replenished from their own H_2/O_2 radical pool as they react. These are sufficient to fully drain the hydrocarbon radicals and so prevent the possibility of soot formation. In richer flames, the residual levels of O_2 and O are small and the oxidation drainage rate much reduced. At $\phi = 2$ in the present case with O_2 (3.4 ppmv) and O (15 ppmv), the flames hydrogen/oxygen pool is still largely in balance except that the oxidation drain to CO is negligible. In such cases, the hydrocarbon radical pool now has the potential to be much longer-lived. Moreover, this now provides the environment for the hydrocarbon−hydrocarbon reactions to step in and begin to display their influence. They now become the main drain of the still very dynamic hydrocarbon pool and initiate the growth of the aromatic soot precursors. Because there is a richness of larger stable C/H/O hydrocarbon radicals that can form, it is not too surprising that recombination-type reactions will spawn a complexity of soot precursors. However, the system still is functioning in a very H-atom/H_2-rich reducing environment that is striving to go to equilibrium, which is carbon and H_2. In fact, in the past, such rich flames have been considered as a potential source of H_2.[119,120] A recent extensive review of the suggested growth kinetics that lead to the formation of benzene and naphthalene aromatics now is available.[121] It is their simultaneous or subsequent pyrolysis and reactions in this rich hydrogen environment that then produces soot.

As a result, the analysis clearly illustrates that a hydrocarbon radical pool will be rapidly established in these atmospheric pressure acetylene flames. Its lifetime is critically controlled by the equivalence ratio. It is this pooling and sharing of the available reactive remaining carbon between the hydrocarbon radicals that provides the connection between CH and C_2. Moreover, the sensitivity to equivalence ratio reflects directly into the effects seen on soot formation of adding oxygenated species or fuels to flames.[122,123] In such cases, added oxygen needs to be factored carefully into an exact calculation of local equivalence ratios.

The Kinetic Consequences for CH, C_2, and Other Hydrocarbon Species. The existence of a hydrocarbon radical pool explains in a very satisfactory and consistent manner the profile data for CH and C_2 in Figures 6 and 7. The decays reflect and track the demise of the full hydrocarbon radical pool. The distribution of hydrocarbon radicals in the pool is a consequence of the numerous reaction rate constants, temperatures, and specific flame species concentrations. These do change but only slightly over the present time regime. Consequently, the two sets of profiles do not have to mirror each other exactly but will be similar. They should closely track though as the distribution modifies.

For $\phi = 1.2$ flames, rates of oxidation and depletion of the hydrocarbon pool are very significant, and the decays are most rapid in the highest temperature $C_2H_2/O_2/N_2$ (1.2/2.5/10, 2380 K) flame. Lowering temperatures conserves the pool longer, and we see a lengthening of its lifetime. As flames become richer, O_2 and O levels are smaller, oxidation rates fall, and lifetimes lengthen. With the change from $\phi = 1.6$ to the $\phi = 2.0$ flame, O_2 and O concentrations decrease by a further 80- and 20-fold, respectively. For $\phi = 2.0$, a dramatic change is noted in the decay rates. Instead of disappearing within 0.5 ms, CH and C_2 extend to their detection limits at 2.5 and 1.5 ms, respectively. Moreover, the decay shape changes and is a more gradual falloff rather than precipitous. It is consistent with a change in the nature of the radical pool drainage mechanism and a move toward the onset of soot formation.

Such a radical pool has mechanistic implications. It has long been recognized even with C_1 fuels such as CH_4 that C_2H_2 and other bicarbon radicals are rapidly formed in the burned gases.[124−127] As observed in the Figure 8 network, the chemistry that couples C_2 to C_1 chemistries is well established, and CH_2-CO, CHCO, and C_2O all react efficiently with H atom to facilitate this. However, the reverse coupling is more limited and has always been assumed to be via CH_3 recombination or its reaction with other single carbon radicals.[126,128,129] As stressed above, for such reactions to compete in this 100−500 μs region of the present flames would require CH_3 concentrations to be large (2%), which is not conceivable in the present flames. There is little doubt that the many reactions ensure a rapid pool formation among the C_1 species and similarly among the C_2

species. However, for the profiles of CH and C_2 to reflect one another, it is additionally necessary for the C_1 and C_2 schemes also to be effectively coupled. Without this, it would appear from Table 4 and Figure 8 that the bicarbon species would rapidly be converted to produce solely a distribution of C_1 hydrocarbon radicals in this region. In the present work, two reactions have been considered to offset this.

$$CH + CO = C_2O + H \qquad \Delta H_{298K} = +114 \text{ kJ mol}^{-1}$$

$$CH_2OH + CO = CH_2CO + OH \qquad \Delta H = +117 \text{ kJ mol}^{-1}$$

Although not considered here, or elsewhere, an additional coupling reaction that also needs further examination in future detailed modeling is the spin-allowed recombination.

$$CH_2(a^1A) + CO + M = CH_2CO + M \qquad \Delta H = -366 \text{ kJ mol}^{-1}$$

If this has a binary rate constant at 2000 K that reflects the value reported at room temperature,[130] the reaction will be important and on a microsecond time scale at atmospheric pressure. Although the two prior reactions above are quite endothermic, as seen in Table 4, the high concentration levels of CO can effectively drive them. The former, listed by Baulch et al.,[74] has only recently been added to the GRI-Mech 3.0 mechanism.[10] Although not considered, the reaction is also plausible and spin-allowed for the metastable $CH(a^4\Sigma^-)$ state for which it becomes only 42 kJ mol^{-1} endothermic. Such a channel has not yet been examined theoretically.[131] The second reaction above appears to be newly suggested herein. Without the possibility of mutual hydrocarbon radical interactions, and to maintain a kinetic linearity, the only reactions that can build from C_1 to C_2 must necessarily invoke CO or CO_2. As a result, there appear to be no other possibilities to suggest that are reasonable.

VII. Conclusions and Implications

Very fast chemistry, as in combustion, is prone to form steady-state distributions. Exactly 50 years ago, Bulewicz, James, and Sugden[68] noted the additional possible consequence that some of these could also couple and form a species pool. In their case of hydrogen flames, the steady-state distribution of radicals and molecules collapsed even further to a simpler partial equilibrium description. The present paper is dedicated to their valuable contribution that has added so much to our understanding of combustion chemistries. Since then, additional species pools have been noted in sulfur combustion[69,132] and in $H_2/F_2/O_2$ combustion.[133] The present work adds a further example but is additionally novel in that it is a radical pool controlled by the more dominant H_2/O_2 pool. In essence, it is "a pool within a pool".

The consequences and implications of the existence of such a hydrocarbon pool near the reaction zone of flames are quite extensive. They can only be mentioned here briefly but may provide the answer for a number of unconnected combustion problems. Additional publications will enlarge on the details elsewhere.

First, a radical pool produces an ordered spread over a distribution. This automatically introduces a certain buffering effect against major change. Variations in one species of a pool will be moderated by the subsequent averaging over the whole. Because of this, additions of new species to a kinetic model describing such a pool may not affect the overall distribution as one might have otherwise expected. As long as most of the major radicals and relevant molecules and their dominant reactions are included in a model, these alone will describe the distribution adequately and it will become increasingly difficult to perturb. Any rush to add newly discovered flame species to models may have little benefit. Consequently, the recent flurry over discovering enols in flames is probably of minor significance to the development of even detailed realistic chemical combustion models.[134−136] A complete degree of exactness of a kinetic model may not be necessary. Also, there can be a loss in kinetic distinguishability and also in kinetic sensitivity. The former relates to being able to clearly identify specific dependences. If radicals are coupled by linear relationships in a way such as H and OH are in most flames, their individual roles in mechanisms cannot be established solely from flame studies. They become indistinguishable in a radical pool. In such cases, information has to be obtained from experimental methods other than flames. Also, the most abundant species in a system do not necessarily imply a major role. It is always possible for a minor species that is coupled to the pool but has very efficient interactions to have the controlling importance. Additionally, the buffering aspects reflect into the systems kinetic sensitivity. An error in a rate constant is averaged over the whole pool and so is minimized. This undoubtedly is the answer to why models with differing databases of rate constants can still reproduce data to similar levels of accuracy. The study by Hughes et al.[137] recently did such an exercise for CH_4 combustion. They compared their model with three other independent mechanisms, one of which was GRI-Mech 3.0.[8] They were surprised by the agreements despite numerous differences including very different rate expressions. This was also noted but 30 years earlier by Creighton.[138] It was also realized by Thoman and McIlroy,[139] who noted that their CH concentration profiles obtained in $\phi = 1.0-1.6$ low-pressure $CH_4/O_2/Ar$ flames could be equally well described by any of four different models. It now appears quite plausible that all of these observations are a consequence of a radical pool. As expressed already, exactness of a mechanism is lessened if a species pool is involved.

In addition, if the rate constants for the dominant channels are known, a steady-state analysis can derive the relative species distribution. Present attempts at this fail as too much uncertainty still remains in the necessary matrix of reaction rate constants. However, in the case of CH, as seen in Table 2, its database of rate constants is quite well established. Consequently, assuming that CH is produced predominantly from CH_2, and equating this to the total loss flux, an approximate ratio of 0.4 at 0.2 ms can be derived for the CH/CH_2 concentrations in any of the three flames listed in Table 2. Norton and Smyth[140] did a similar type analysis with their CH measurements in a methane diffusion flame. Consequently, as is well-known, the concept of steady-state distributions can simplify kinetic modeling and satisfy a general need for reduced kinetic mechanisms.[141]

The early isotopic work of Ferguson[12,142] with ^{13}C labeling and the now several additional ^{14}C- and D-labeled studies all need re-examination.[143,144] For example, one study has noted that, although CH_3OH alone is not prone to soot formation, when labeled and burned in a mixture with toluene then the methanol-labeled carbon also is present in the soot.[145] This was a noteworthy observation that remained unexplained. It would now seem to be readily understood via the radical pool concept outlined herein.

In light of the very fast and efficient hydrocarbon reactions listed in the various tables, it is surprising and hard to understand how the numerous flame studies that have utilized probe

sampling appear to be successful in quantitatively monitoring trace species.[79,124−128,136,146] These generally have sampled low-pressure flames directly into molecular beam mass spectrometers. One study collected samples from atmospheric pressure flames in analysis cells for the subsequent analysis of the C_2H_2 content in CH_4/air flames.[127] This would seem to be totally inconsistent for species that are well established as reacting at the collisional frequency on a sub-microsecond time scale even at reduced pressure. Nevertheless, there is a general acceptance and model validation that the data are sound. If so, it may be that the radicals being locked in a radical pool are an aid in maintaining the distribution through quenching. Even so, this method has to produce some degree of approximation. It seems impossible to instantly freeze all collisions by any means of such sampling. Until they are further analyzed and substantiated by a method other than modeling, such approaches must remain suspect to some degree.

The nature of a hydrocarbon radical pool in the C_1/C_2 radical region appears to be one of linear relationships in that one carbon radical changes into another even in the C_1/C_2 coupling reactions. If so, this can finally offer a more complete mechanism for the FID. It can now be understood as to how the linearly scaled levels of CH are produced in a hydrogen diffusion flame seeded with different hydrocarbon structures. It also becomes apparent why different carbon atoms as in partially oxidized organics such as acetone count as two and not three carbons. This is particularly important at present when considerable efforts are examining the structural effects of oxygenated fuels,[122,123,144,147] which is exactly what the FID is all about and was resolved quite extensively many years ago.[46,148−150]

Another interesting subject impacted by such radical pool concepts is flame-generated diamond formation. This now has a very rich literature that also extends to heated filament, heated tube reactor, microwave, and other plasma discharge techniques.[151] Rather than simplifying an understanding, the vast array of data shows a significant range of conclusions. Although initial models favored CH_3 as the depositing radical, the following species now have each been reported as playing the dominant role in the following studies, C,[152−154] C_2,[155−157] CH,[155,158] CH_2,[152] CH_3,[152,154,159,160] and C_2H.[161] The study of Ashfold et al.[162] was noteworthy in reporting that the composition of the various hydrocarbon species in the vicinity of the surface was independent of the particular hydrocarbon source used. A resolution of these discordant conclusions may now be found in the radical pool that makes these species indistinguishable in high-temperature plasmas.

VIII. Summary

CH and C_2 radicals are the species that have historically been synonymous with hydrocarbon combustion due to their pronounced chemiluminescent emissions that color fossil-fueled flames. Their choice for study proved to be auspicious, as were the specific acetylene flames. The resulting data for their flame profiles were immediately intriguing due to their strikingly similar appearances. A connection between the two was obviously apparent but not easy to explain. Coupled to other reports, it did seem as though the data were reflecting the possibility of some underlying simplicity in these otherwise very complex systems. As a result, a detailed analysis of the chemical kinetics was undertaken specifically for this limited time frame, within which they are observed. In the flames studied, this extends from the reaction zone for only the first several hundreds of microseconds into the burned gases. The task was to find how the two radicals could be interrelated in some way and whether they have any specific importance. Only one solution emerged but with such additional implications that it immediately appeared to be self-validating, that these radicals together with the majority of the other hydrocarbon fragments have steady-state distributions that become rapidly locked in a radical pool. It is this pooling that finally explains how two such chemically different species as these that lie in different sections of any kinetic network can be related and have an ability to track one another.

The lifetime of the radical pool is very dependent on equivalence ratios. With sufficient oxygen it is drained rapidly. However, with fuel richness the draining by oxidation becomes negligible, and as the soot inception ratios are approached then radicals are no longer drained by oxidation but by mutual radical recombination. Moreover, all of the time the pool is operating under the control of the larger radical pool of the H_2/O_2 system. It is truly a radical pool within a pool. As to importance, it might be stated that CH and C_2 both are important. However, this can be said for all of the radicals within the pool. They share equally their ever-changing part of the available pool of remaining unburned carbon. In this way, as once hinted,[13,14] all of the carbon can be regarded as processing through CH or C_2. However, as to their individual importance in, for example, chemi-ionization, NO_x, or soot formation, this cannot be rigorously established from solely flame studies. The nature of the pool is to disguise their individuality in flames, and so external confirmation is additionally required.

As summarized in the previous section, these findings now appear to have implications in other combustion areas. Some will be addressed separately in the near future.

Acknowledgment. This paper is dedicated to the memory of Sir T. M. (Morris) Sugden, FRS, and commemorating his paper with E. M. Bulewicz and C. G. James published 50 years ago.[68] These authors discovered the first radical pool in hydrogen flames, which helped lay a foundational understanding of combustion chemistry. This work initially was made possible by a grant from the Engineering Division of Chemical and Process Engineering, National Science Foundation, Washington, DC20550, under Grant Number NSF CPE 84-12951. It was performed in the Quantum Institute of the University of California, Santa Barbara. It would not have been completed without the financial support from the Robinson-Schofield Foundation.

References and Notes

(1) Miller, J. A.; Pilling, M. J.; Troe, J. *Proc. Combust. Inst.* **2005**, *30*, 43.

(2) Peeters, J.; Vinckier, C. *Proc. Combust. Inst.* **1974**, *15*, 969.

(3) Berg, P. A.; Hill, D. A.; Noble, A. R.; Smith, G. P.; Jeffries, J. B.; Crosley, D. R. *Combust. Flame* **2000**, *121*, 223.

(4) Basevich, V. Ya. *Prog. Energy Combust. Sci.* **1987**, *13*, 199.

(5) Lindstedt, R. P.; Skevis, G. *Combust. Sci. Technol.* **1997**, *125*, 73.

(6) Wang, H.; Frenklach, M. *Combust. Flame* **1997**, *110*, 173.

(7) Varatharajan, B.; Williams, F. A. *Combust. Flame* **2001**, *124*, 624.

(8) Smith, G. P.; Golden, D. M.; Frenklach, M.; Moriarty, N. W.; Eiteneer, B.; Goldenberg, M.; Bowman, C. T.; Hanson, R. K.; Song, S.; Gardiner, W. C., Jr.; Lissianski, V. V.; Qin, Z. *GRI-Mech 3.0*; http://www.me.berkeley.edu/gri_mech/.

(9) Bernstein, J. S.; Fein, A.; Choi, J. B.; Cool, T. A.; Sausa, R. C.; Howard, S. L.; Locke, R. J.; Miziolek, A. W. *Combust. Flame* **1993**, *92*, 85.

(10) Smith, G. P.; Park, C.; Schneiderman, J.; Luque, J. *Combust. Flame* **2005**, *141*, 66.

(11) Brockhinke, A.; Letzgus, M.; Rinne, S.; Kohse-Hoinghaus, K. *J. Phys. Chem. A* **2006**, *110*, 3028.

(12) Ferguson, R. E. *J. Chem. Phys.* **1955**, *23*, 2085.

(13) Darian, S. T.; Vanpee, M. *Combust. Flame* **1987**, *70*, 65.

(14) Gaydon, A. G.; Wolfhard, H. G. *Flames: Their Structure, Radiation and Temperature*, 3rd ed.; Chapman & Hall: London, 1970.
(15) Smyth, K. C.; Crosley, D. R. In *Applied Combustion Diagnostics*; Kohse-Hoinghaus, K., Jeffries, J. B., Eds.; Taylor & Francis: New York, 2002; pp 9−68.
(16) Bleekrode, R.; Nieuwpoort, W. C. *J. Chem. Phys.* **1965**, *43*, 3680.
(17) Bleekrode, R. *Phillips Res. Rep.* **1967**, Suppl. 7.
(18) Porter, R. P.; Clark, A. H.; Kaskan, W. E.; Browne, W. E. *Proc. Combust. Inst.* **1966**, *11*, 907.
(19) Jessen, P. F.; Gaydon, A. G. *Proc. Combust. Inst.* **1968**, *12*, 481.
(20) Bulewicz, E. M.; Padley, P. J.; Smith, R. E. *Proc. R. Soc. London, Ser. A* **1970**, *315*, 129.
(21) Guillaume, P.; Van Tiggelen, P. J. *Proc. Combust. Inst.* **1984**, *20*, 751.
(22) Goldsmith, J. E. M.; Kearsley, D. T. B. *Appl. Phys. B* **1990**, *50*, 371.
(23) Williams, B. A.; Pasternack, L. *Combust. Flame* **1997**, *111*, 87.
(24) Joklik, R. G.; Daily, J. W.; Pitz, W. J. *Proc. Combust. Inst.* **1986**, *21*, 895.
(25) Kohse-Hoinghaus, K.; Kelm, S.; Meier, U.; Bittner, J.; Just, T. *Springer Ser. Chem. Phys.* **1987**, *47*, 292.
(26) Miller, J. A.; Volponi, J. V.; Durant, J. L., Jr.; Goldsmith, J. E. M.; Fisk, G. A.; Kee, R. J. *Proc. Combust. Inst.* **1990**, *23*, 187.
(27) Volponi, J. V.; Branch, M. C. *Proc. Combust. Inst.* **1992**, *24*, 823.
(28) Miller, J. A.; Volponi, J. V.; Pauwels, J.-F. *Combust. Flame* **1996**, *105*, 451.
(29) Westbrook, C. K.; Mizobuchi, Y.; Poinsot, T. J.; Smith, P. J.; Warnatz, J. *Proc. Combust. Inst.* **2005**, *30*, 125.
(30) Buckmaster, J.; Clavin, P.; Linan, A.; Matalon, M.; Peters, N.; Sivashinsky, G.; Williams, F. A. *Proc. Combust. Inst.* **2005**, *30*, 1.
(31) Miller, J. A.; Melius, C. F. *Combust. Flame* **1992**, *91*, 21.
(32) Eiteneer, B.; Frenklach, M. *Int. J. Chem. Kinet.* **2003**, *35*, 391.
(33) Hoyermann, K.; Mauss, F.; Zeuch, T. *Phys. Chem. Chem. Phys.* **2004**, *6*, 3824.
(34) Maas, U.; Pope, S. B. *Combust. Flame* **1992**, *88*, 239.
(35) Yang, B.; Pope, S. B. *Combust. Flame* **1998**, *112*, 16.
(36) Skodje, R. T.; Davis, M. J. *J. Phys. Chem. A* **2001**, *105*, 10356.
(37) Konig, K.; Maas, U. *Proc. Combust. Inst.* **2005**, *30*, 1317.
(38) Lu, T.; Ju, Y.; Law, C. K. *Combust. Flame* **2001**, *126*, 1445.
(39) Lam, S. H.; Goussis, D. A. *Proc. Combust. Inst.* **1988**, *22*, 931.
(40) Valorani, M.; Creta, F.; Goussis, D. A.; Lee, J. C.; Najm, H. N. *Combust. Flame* **2006**, *146*, 29.
(41) Montgomery, C. J.; Yang, C.; Parkinson, A. R.; Chen, J.-Y. *Combust. Flame* **2006**, *144*, 37.
(42) Oluwole, O. O.; Bhattacharjee, B.; Tolsma, J. E.; Barton, P. I.; Green, W. H. *Combust. Flame* **2006**, *146*, 348.
(43) Warnatz, J.; Bockhorn, H.; Moser, A.; Wenz, H. W. *Proc. Combust. Inst.* **1982**, *19*, 197.
(44) McWilliam, I. G.; Dewar, R. A. *Nature* **1958**, *181*, 760.
(45) McWilliam, I. G.; Dewar, R. A. In *Gas Chromatography: Proceedings of the 2nd Symposium*; Desty, D. H., Ed.; Butterworths Scientific Publications: London, 1958; pp 142−152.
(46) Sternberg, J. C.; Gallaway, W. S.; Jones, D. T. L. In *Gas Chromatography: Proceedings of the 3rd International Symposium*; Brenner, N., Callen, J. E., Weiss, M. D., Eds.; Academic Press: New York, 1962; pp 231−267.
(47) Bulewicz, E. M.; Padley, P. J. *Proc. Combust. Inst.* **1962**, *9*, 638.
(48) Dietz, W. A. *J. Gas Chromatogr.* **1967**, *5*, 68.
(49) Blades, A. T. *J. Chromatogr. Sci.* **1973**, *11*, 251.
(50) Calcote, H. F. *Proc. Combust. Inst.* **1960**, *8*, 184.
(51) Nicholson, A. J. C. *J. Chem. Soc., Faraday Trans. 1* **1982**, *78*, 2183.
(52) Holm, T.; Madsen, J. O. *Anal. Chem.* **1996**, *68*, 3607.
(53) Holm, T. *J. Chromatogr., A* **1997**, *782*, 81.
(54) Holm, T. *J. Chromatogr., A* **1999**, *842*, 221.
(55) Wagner, J. H.; Lillie, C. H.; Dupuis, M. D.; Hill, H. H., Jr. *Anal. Chem.* **1980**, *52*, 1614.
(56) Fairbairn, A. R. *Proc. R. Soc. London, Ser. A* **1969**, *312*, 229.
(57) Beck, W. H.; Mackie, J. C. *J. Chem. Soc., Faraday Trans. 1* **1975**, *71*, 1363.
(58) Sommer, T.; Kruse, T.; Roth, P. *J. Phys. Chem.* **1995**, *99*, 13509.
(59) Levy, M. R.; Reisler, H.; Mangir, M. S.; Wittig, C. *Opt. Eng.* **1980**, *19*, 29.
(60) Hetherington, W. M., III; Korenowski, G. M.; Eisenthal, K. B. *Chem. Phys. Lett.* **1981**, *77*, 275.
(61) Craig, B. B.; Faust, W. L.; Goldberg, L. S.; Weiss, R. G. *J. Chem. Phys.* **1982**, *76*, 5014.
(62) Li, Z.; Francisco, J. S. *J. Chem. Phys.* **1992**, *96*, 878.
(63) Bengtsson, P.-E.; Alden, M. *Combust. Flame* **1990**, *80*, 322.
(64) Mercier, X.; Therssen, E.; Pauwels, J. F.; Desgroux, P. *Proc. Combust. Inst.* **2005**, *30*, 1655.
(65) Chou, M.-S.; Dean, A. M. *Int. J. Chem. Kinet.* **1985**, *17*, 1103.
(66) Muller, C. H., III; Schofield, K.; Steinberg, M. *Am. Chem. Soc. Symp. Ser.* **1980**, *134*, 103.
(67) Hynes, A. J.; Steinberg, M.; Schofield, K. *J. Chem. Phys.* **1984**, *80*, 2585.
(68) Bulewicz, E. M.; James, C. G.; Sugden, T. M. *Proc. R. Soc. London, Ser. A* **1956**, *235*, 89.
(69) Muller, C. H., III; Schofield, K.; Steinberg, M.; Broida, H. P. *Proc. Combust. Inst.* **1978**, *17*, 867.
(70) Bass, A. M.; Broida, H. P. *A Spectrophotometric Atlas of the Spectrum of CH from 3000 to 5000 A*; U.S. Department of Commerce, National Bureau of Standards Monograph 24, 1961.
(71) Moore, C. E.; Broida, H. P. *J. Res. Natl. Bur. Stand., Sect. A* **1959**, *63*, 19.
(72) Phillips, J. G.; Davis, S. P. *The Swan System of the C_2 Molecule*; University of California Press: Berkeley, CA, 1968.
(73) Gordon, S.; McBride, B. J. *Computer Program for Calculation of Complex Chemical Equilibrium Compositions and Applications. I. Analysis. II. Users Manual and Program Description*; NASA Lewis Research Center, Reference Publication NASA RP-1311, Part I, 1994; NASA RP 1311, Part II, 1996.
(74) Baulch, D. L.; Bowman, C. T.; Cobos, C. J.; Cox, R. A.; Just, Th.; Kerr, J. A.; Pilling, M. J.; Stocker, D.; Troe, J.; Tsang, W.; Walker, R. W.; Warnatz, J. *J. Phys. Chem. Ref. Data* **2005**, *34*, 757.
(75) Fenimore, C. P.; Jones, G. W. *J. Phys. Chem.* **1958**, *62*, 693.
(76) Reid, R.; Wheeler, R. *J. Phys. Chem.* **1961**, *65*, 527.
(77) Levy, J. M.; Taylor, B. R.; Longwell, J. P.; Sarofim, A. F. *Proc. Combust. Inst.* **1982**, *19*, 167.
(78) Levy, J. M.; Sarofim, A. F. *Combust. Flame* **1983**, *53*, 1.
(79) Bittner, J. D.; Howard, J. B. *Proc. Combust. Inst.* **1982**, *19*, 211.
(80) Burgess, A. R.; Langley, C. J. *Proc. R. Soc. London, Ser. A* **1991**, *433*, 1.
(81) Chase, M. W., Jr.; Davies, C. A.; Downey, J. R., Jr.; Frurip, D. J.; McDonald, R. A.; Syverud, A. N. *JANAF Thermochemical Tables, Third Edition*, *J. Phys. Chem. Ref. Data* **1985**, *14*, Suppl. 1.
(82) Ni, T.; Nie, X.; Yu, S.; Kong, F. *Sci. Sin., Ser. B* **1988**, *31*, 926.
(83) Gurvich, L. V.; Veyts, I. V.; Alcock, C. B. *Thermodynamic Properties of Individual Substances*, 4th ed.; Hemisphere Publishing Corp.: New York, 1991; Vol. 2.
(84) Ruscic, B.; Boggs, J. E.; Burcat, A.; Csaszar, A. G.; Demaison, J.; Janoschek, R.; Martin, J. M. L.; Morton, M. L.; Rossi, M. J.; Stanton, J. F.; Szalay, P. G.; Westmoreland, P. R.; Zabel, F.; Berces, T. *J. Phys. Chem. Ref. Data* **2005**, *34*, 573.
(85) Chuang, M.-C.; Foltz, M. F.; Moore, C. B. *J. Chem. Phys.* **1987**, *87*, 3855.
(86) Becerra, R.; Carpenter, I. W.; Walsh, R. *J. Phys. Chem. A* **1997**, *101*, 4185.
(87) Matus, M. H.; Nguyen, M. T.; Dixon, D. A. *J. Phys. Chem. A* **2006**, *110*, 8864.
(88) Urdahl, R. S.; Bao, Y.; Jackson, W. M. *Chem. Phys. Lett.* **1991**, *178*, 425.
(89) Mordaunt, D. H.; Ashfold, M. N. R. *J. Chem. Phys.* **1994**, *101*, 2630.
(90) Osborn, D. L.; Mordaunt, D. H.; Choi, H.; Bise, R. T.; Neumark, D. M.; Rohlfing, C. M. *J. Chem. Phys.* **1997**, *106*, 10087.
(91) Jursic, B. S. *Int. J. Quantum Chem.* **1999**, *72*, 571.
(92) Hayakawa, S.; Tomozawa, K.; Takeuchi, T.; Arakawa, K.; Morishita, N. *Phys. Chem. Chem. Phys.* **2003**, *5*, 2386.
(93) Choi, H.; Mordaunt, D. H.; Bise, R. T.; Taylor, T. R.; Neumark, D. M. *J. Chem. Phys.* **1998**, *108*, 4070.
(94) Gurvich, L. V.; Veyts, I. V.; Alcock, C. B. *Thermodynamic Properties of Individual Substances*, 4th ed.; Hemisphere Publishing Corp.: New York, 1989; Vol. 1.
(95) Ruscic, B.; Litorja, M. *Chem. Phys. Lett.* **2000**, *316*, 45.
(96) Flowers, B. A.; Szalay, P. G.; Stanton, J. F.; Kallay, M.; Gauss, J.; Csaszar, A. G. *J. Phys. Chem. A* **2004**, *108*, 3195.
(97) Ruscic, B.; Pinzon, R. E.; Morton, M. L.; Srinivasan, N. K.; Su, M.-C.; Sutherland, J. W.; Michael, J. V. *J. Phys. Chem. A* **2006**, *110*, 6592.
(98) Zhang, X.; Ding, Y.-h.; Li, Z.-s.; Huang, X.-r.; Sun, C.-c. *Chem. Phys. Lett.* **2000**, *330*, 577.
(99) Wang, J.-H.; Han, K.-L.; He, G.-Z.; Li, Z.; Morris, V. R. *J. Phys. Chem. A* **2003**, *107*, 9825.
(100) Kruse, T.; Roth, P. *Proc. Combust. Inst.* **1998**, *27*, 193.
(101) Hwang, D.-Y.; Mebel, A. M.; Wang, B.-C. *Chem. Phys.* **1999**, *244*, 143.
(102) Xia, W. S.; Zhu, R. S.; Lin, M. C.; Mebel, A. M. *Faraday Discuss.* **2001**, *119*, 191.
(103) Krasnoperov, L. N.; Michael, J. V. *J. Phys. Chem. A* **2004**, *108*, 8317.
(104) Hayes, F.; Lawrance, W. D.; Staker, W. S.; King, K. D. *J. Phys. Chem.* **1996**, *100*, 11314.
(105) Lissi, E. A.; Massiff, G.; Villa, A. E. *J. Chem. Soc., Faraday Trans. 1* **1973**, *69*, 346.
(106) Fockenberg, C.; Preses, J. M. *J. Phys. Chem. A* **2002**, *106*, 2924.

(107) Xu, S.; Zhu, R. S.; Lin, M. C. *Int. J. Chem. Kinet.* **2006**, *38*, 322.
(108) Bauerfeldt, G. F.; de Albuquerque, L. M. M.; Arbilla, G.; da Silva, E. C. *J. Mol. Struct. (THEOCHEM)* **2002**, *580*, 147.
(109) Feng, L.; Reisler, H. *J. Phys. Chem. A* **2004**, *108*, 9847.
(110) Curran, H. J. *Int. J. Chem. Kinet.* **2006**, *38*, 250.
(111) Seetula, J. A.; Kalinovski, I. J.; Slagle, I. R.; Gutman, D. *Chem. Phys. Lett.* **1994**, *224*, 533.
(112) Xu, S.; Lin, M. C. *Proc. Combust. Inst.* **2007**, *31*, 159.
(113) Senosiain, J. P.; Klippenstein, S. J.; Miller, J. A. *J. Phys. Chem. A* **2005**, *109*, 6045.
(114) Carl, S. A.; Nguyen, H. M. T.; Elsamra, R. M. I.; Nguyen, M. T.; Peeters, J. *J. Chem. Phys.* **2005**, *122*, 114307.
(115) Nguyen, T. L.; Vereecken, L.; Peeters, J. *J. Phys. Chem. A* **2006**, *110*, 6696.
(116) Carl, S. A.; Sun, Q.; Teugels, L.; Peeters, J. *Phys. Chem. Chem. Phys.* **2003**, *5*, 5424.
(117) Hou, H.; Wang, B.; Gu, Y. *Phys. Chem. Chem. Phys.* **2000**, *2*, 2329.
(118) Schocker, A.; Kohse-Hoinghaus, K.; Brockhinke, A. *Appl. Opt.* **2005**, *44*, 6660.
(119) Lewis, D. H., Jr. *Combust. Flame* **1981**, *42*, 105.
(120) Warchol, J. J.; Reuther, J. J. *Combust. Flame* **1984**, *55*, 341.
(121) McEnally, C. S.; Pfefferle, L. D.; Atakan, B.; Kohse-Hoinghaus, K. *Prog. Energy Combust. Sci.* **2006**, *32*, 247.
(122) Kaiser, E. W.; Wallington, T. J.; Hurley, M. D.; Platz, J.; Curran, H. J.; Pitz, W. J.; Westbrook, C. K. *J. Phys. Chem. A* **2000**, *104*, 8194.
(123) Westbrook, C. K.; Pitz, W. J.; Curran, H. J. *J. Phys. Chem. A* **2006**, *110*, 6912.
(124) Miller, J. H.; Mallard, W. G.; Smyth, K. C. *Proc. Combust. Inst.* **1986**, *21*, 1057.
(125) Crunelle, B.; Pauwels, J. F.; Sochet, L. R. *Bull. Soc. Chim. Belg.* **1996**, *105*, 491.
(126) Musick, M.; Van Tiggelen, P. J.; Vandooren, J. *Combust. Flame* **1996**, *105*, 433.
(127) Gersen, S.; Mokhov, A. V.; Levinsky, H. B. *Combust. Flame* **2005**, *143*, 333.
(128) Hennessy, R. J.; Robinson, C.; Smith, D. B. *Proc. Combust. Inst.* **1986**, *21*, 761.
(129) Ranzi, E.; Sogaro, A.; Gaffuri, P.; Pennati, G.; Faravelli, T. *Combust. Sci. Technol.* **1994**, *96*, 279.
(130) Langford, A. O.; Petek, H.; Moore, C. B. *J. Phys. Chem.* **1983**, *78*, 6650.
(131) Yarkony, D. R. *J. Phys. Chem.* **1996**, *100*, 17439.
(132) Cerru, F. G.; Kronenburg, A.; Lindstedt, R. P. *Proc. Combust. Inst.* **2005**, *30*, 1227.
(133) Creighton, J. R.; Oppenheim, A. K. *Prog. Astro. Aeronaut.* **1986**, *105-PartII*, 304.
(134) Cool, T. A.; Nakajima, K.; Mostefaoui, T. A.; Qi, F.; Mcllroy, A.; Westmoreland, P. R.; Law, M. E.; Poisson, L.; Peterka, D. S.; Ahmed, M. *J. Chem. Phys.* **2003**, *119*, 8356.
(135) Taatjes, C. A.; Hansen, N.; Mcllroy, A.; Miller, J. A.; Senosiain, J. P.; Klippenstein, S. J.; Qi, F.; Sheng, L.; Zhang, Y.; Cool, T. A.; Wang, J.; Westmoreland, P. R.; Law, M. E.; Kasper, T.; Kohse-Hoinghaus, K. *Science* **2005**, *308*, 1887.
(136) Taatjes, C. A.; Hansen, N.; Miller, J. A.; Cool, T. A.; Wang, J.; Westmoreland, P. R.; Law, M. E.; Kasper, T.; Kohse-Hoinghaus, K. *J. Phys. Chem. A* **2006**, *110*, 3254.
(137) Hughes, K. J.; Turanyi, T.; Clague, A. R.; Pilling, M. J. *Int. J. Chem. Kinet.* **2001**, *33*, 513.
(138) Creighton, J. R. *J. Phys. Chem.* **1977**, *81*, 2520.
(139) Thoman, J. W., Jr.; McIlroy, A. *J. Phys. Chem. A* **2000**, *104*, 4953.
(140) Norton, T. S.; Smyth, K. C. *Combust. Sci. Technol.* **1991**, *76*, 1.
(141) *Reduced Kinetic Mechanisms for Applications in Combustion Systems*; Peters, N., Rogg, B., Eds.; Lect. Notes Phys.: Monograph 15; Springer-Verlag: New York, 1993.
(142) Ferguson, R. E. *Combust. Flame* **1957**, *1*, 431.
(143) Homan, H. S.; Robbins, W. K. *Combust. Flame* **1986**, *63*, 177.
(144) Buchholz, B. A.; Mueller, C. J.; Upatnieks, A.; Martin, G. C.; Pitz, W. J.; Westbrook, C. K. Using Carbon-14 Isotope Tracing to Investigate Molecular Structure Effects of the Oxygenate Dibutyl Maleate on Soot Emissions from a Direct Injection Diesel Engine, SAE Paper 2004-01-1849. *New Combustion Systems in Spark Ignition and Diesel Engines, and Combustion and Emission Formation Processes in Diesel Engines*; Special Publication SP-1890, 2004; pp 143−154.
(145) Sorek, H.; Anderson, J. E. *Combust. Sci. Technol.* **1985**, *43*, 321.
(146) Bastin, E.; Delfau, J.-L.; Reuillon, M.; Vovelle, C.; Warnatz, J. *Proc. Combust. Inst.* **1988**, *22*, 313.
(147) Fisher, E. M.; Pitz, W. J.; Curran, H. J.; Westbrook, C. K. *Proc. Combust. Inst.* **2000**, *28*, 1579.
(148) Perkins, G., Jr.; Rouayheb, G. M.; Lively, L. D.; Hamilton, W. C. In *Gas Chromatography: Proceedings of the 3rd International Symposium*; Brenner, N., Callen, J. E., Weiss, M. D., Eds.; Academic Press: New York, 1962; pp 269−285.
(149) Ackman, R. G. *J. Gas Chromatogr.* **1968**, *6*, 497.
(150) Morvai, M.; Palyka, I.; Molnar-Perl, I. *J. Chromatogr. Sci.* **1992**, *30*, 448.
(151) *Synthetic Diamond: Emerging CVD Science and Technology*; Spear, K. E., Dismukes, J. P., Eds.; John Wiley: New York, 1994.
(152) Yu, B. W.; Girshick, S. L. *J. Appl. Phys.* **1994**, *75*, 3914.
(153) Wolden, C. A.; Davis, R. F.; Sitar, Z.; Prater, J. T. *J. Mater. Res.* **1997**, *12*, 2733.
(154) Ruf, B.; Behrendt, F.; Deutschmann, O.; Kleditzsch, S.; Warnatz, J. *Proc. Combust. Inst.* **2000**, *28*, 1455.
(155) Welter, M. D.; Menningen, K. L. *J. Appl. Phys.* **1997**, *82*, 1900.
(156) McCauley, T. G.; Gruen, D. M.; Krauss, A. R. *Appl. Phys. Lett.* **1998**, *73*, 1646.
(157) Klein-Douwel, R. J. H.; ter Meulen, J. J. *J. Appl. Phys.* **1998**, *83*, 4734.
(158) Stolk, R. L.; ter Meulen, J. J. *Diamond Relat. Mater.* **1999**, *8*, 1251.
(159) D'Evelyn, M. P.; Chu, C. J.; Hauge, R. H.; Margrave, J. L. *J. Appl. Phys.* **1992**, *71*, 1528.
(160) Wu, J.-J.; Hong, F. C.-N. *Appl. Phys. Lett.* **1997**, *70*, 185.
(161) Rau, H.; Picht, F. *J. Mater. Res.* **1993**, *8*, 2250.
(162) Ashfold, M. N. R.; May, P. W.; Petherbridge, J. R.; Rosser, K. N.; Smith, J. A.; Mankelevich, Y. A.; Suetin, N. V. *Phys. Chem. Chem. Phys.* **2001**, *3*, 3471.